NIRS
HIMAC

NIRS-M-112
HIMAC-012

Synchrotron Power Supply of Sub-ppm Ripple Current

M. KUMADA, K. SATO, S. MATSUMOTO,
K. NODA and E. TAKADA

January 1996

National Institute of Radiological Sciences

4-9-1, Anagawa, Inage-ku, Chiba 263 JAPAN

Synchrotron Power Supply of Sub-ppm Ripple Current

Masayuki Kumada
National Institute of Radiological Sciences
4-9-1 Anagawa, Inage, Chiba, Japan
(e-mail) kumada@nirs.go.jp

Abstract

Synchrotrons have long been undergoing a non-negligible ripple current during a slow beam extraction. Non-uniform beam spill is attributed to non-negligible quantity of logical and illogical harmonic ripple and thyristor spike of the main power supply. Requirements for the synchrotron power supply are a stability, a reproducibility, a constant ratio of the magnet field among Quadrupole magnets and Bending magnets, and homogeneity in time domain. Among others, the most demanding requirement for the resonant slow beam extraction is to suppress the ripple to a negligible amount. The goal has been to achieve a level of several ppm or lower in a relative content of the ripple current. However, it has not been realized by the power supply alone. In the HIMAC synchrotron, we have achieved a level below ppm both for the power supply of the main Quadrupole and the Bending magnet. Performance is mostly due to a bridge resistor, a separate connection of the upper and lower coil of the magnet and a low pass mode filter that consists of two orthogonal components of the normal and the common mode filter. This article describes the design principle and the performance of the power supply of the HIMAC at NIRS. Theoretical bases are given in an accompanying paper.

I. Introduction

In many slow cycling synchrotrons, excitation current of the magnet string has a trapezoidal form. In particular, the ripple content at the flat top of the trapezoid must be low as possible and should be a few ppm(10^{-6}, parts per million) or less[1]. Requirement for lower ripple is increasing [2]. Trapezoidal form among the power supplies also must be tracked down precisely. In this research, the goal is to find systematic ways to achieve a synchrotron power supply of a relative ripple current below ppm level.

In the HIMAC as for most synchrotrons, a thyristor controlled power supply is used, where high power of several MVA is required. For medium power, the switch mode type of power converter may be recently in use[3]. Thyristor controlled power supply has merits of stable and reliable high power handling capability, variable power factor from 0 to 0.8, having large magnetic elements and moderate prices and competitive market. As a switching semiconductor of power element, thyristor is superior in low forward voltage drop, low leak current, a resistance in high reverse voltage, fast repeatable on-off switching, reliable turning on with small signal, compact size and a long life[5]. Simultaneously, the thyristor controlled power supply is known to suffer from the production of large residual ripple and spike voltage unless proper filtering system is employed. The ripple and spike are composed of several sources of different origins as described in the following.

Ripple and Spike

Basic ripple frequency f_b=1200 Hz of the power supply is given by the frequency of the power sources (f_0=50Hz) multiplied by the number of thyristor pulses (24 in the HIMAC). The Fourier analysis of the ripple voltage also gives multiples of f_b. These ripple components are called logical ripples as they are produced even without hardware imperfections. They are sometimes called as harmonics. A second type of ripples with the frequency of $2nf_0$(n is an integer) are caused by imbalances of the rectifier transformers and by variations in the firing or the extinction of the thyristors. These ripple components are called illogical ripples as they only exist in a presence of hardware imperfections. They are sometimes called as sub-harmonics in a literature. In the HIMAC, the basic frequency of the illogical ripple is 100 Hz. A third type of ripple with the frequencies of f_0, 50 Hz, is caused by the feedback system whose source of ripple is in the low level circuit of the power supply control system. Furthermore oscillatory spike voltage is induced when each of the thyristor is turned on and off as a transient response of the power supply system. The oscillation frequency of the spike ranges between a few kHz and tens of kHz and the duration is less than 1 msec. This spike has been one of the performance limiting factors in thyristor controlled power supply. Amplitude modulated spikes can also contribute ripple at frequencies as low as 100 Hz. A major problem associated with the spike is the production of noise spikes in equipment

located in the neighborhood. These noise effects the reliable performance of the feedback circuit of the power supply itself. In addition to those ripples, there are ripples those frequencies are one half of the frequencies mentioned above. These ripples are called common mode ripples where the definition of the common will be given in subsequent chapters in this article.

Extensive studies have been done by many researchers in developing and improving the performance of the synchrotron power supply. In the following, some of those studies which are related to this article are briefly described.

Basic Approach

Previous studies have been concentrated mainly on the ripple related to illogical ripples. They tried to improve an imbalance [4] among phases of primary AC voltages and to equalize the timing of firing pulses of each thyristor [6,7,8]. They have developed an active filter [9,10,11] and a bandpass filter [12,13] to further reduce this ripple. Setting up an external signal generator in a control circuit as an open loop ripple correction system was another approach for this purpose. An improvement of a factor of 15 was reported at Saclay[14]. We developed a similar device, which we called "Ripple Basher". This was shown to be useful for the study of the relation between the spill performance and the ripple as well as suppressing the ripple. The ripple basher is implemented in an open loop and therefore is very effective for a synchrotron with fixed extraction energy.

Many researchers tried to suppress the spike and ripple between a rectifier and a load by inserting an improved low pass filter. The Praeg type filter[15], where the main capacitor that is supplemented by an additional parallel capacitor with a resistor connected in series, is widely used in most synchrotron power supplies today for the synchrotron of the low ripple content. The performance of the filter also depends on the cut-off frequency of the filter. The cut-off frequency usually ranges between 25 Hz and 100 Hz. Although the higher the cut-off frequency, the better the performance of the filter, there is a trade-off between the cut-off frequency and the tracking capability of the power supply.

In spite of these efforts, the reduction of current spike and ripple has been unsatisfactory for the requirement of the tolerance of the third order resonant extraction, which is at a level of a few ppm or less. The causes of unsatisfactory performance is sometimes ascribed to a poor frequency

characteristic of the elements such as the reactor transformer of the filter or an insufficient accuracy of the voltage and current monitoring system.

The efforts mentioned are partly successful but the performance achieved for the ripple still did not satisfy the required level. To fulfill the requirement for beam extraction, for most of the accelerator in operation, additional means had to be used which are independent of the main power supply, such as spill feedback controller systems with a fast air-core quadrupole magnet or other devices. Thus new approaches are required.

Stray Capacitance in Power Supplies

It was pointed out that the stray capacitor of the transformers, the reactors, cables and other elements is important in considering ripple and spike[16]. The effect of the stray capacitance of the transformer of the rectifier is considered in Figure1, where the stray capacitance of the rectifier is shown as C_G. In most of the existing power supply systems, the thyristor bank is isolated from the ground to avoid noises. The isolation means the neutral point of the thyristor bank has a stray capacitance to the ground. If one could make the stray capacitance to a very small amount, ripple of spike current would be small. The lower the capacitance, the smaller the ripple current. The current drives the potential of the neutral point O in Figure1. However, there is a practical limit of reducing the stray capacitance. In the presence of non-negligible amount of capacitance, high frequency ripple or spike current can flow through the stray capacitance.

A novel attempt is to control the ground potential by setting up an active element between the neutral point and the earth and to control the potential of the neutral point[17]. Their performance for the relative ripple is 10 ppm with DC operation.

A presence of a leakage capacitance or a fluctuation of a potential of the thyristor's neutral point suggested a mechanism discussed in this article that the researchers have overlooked in considering the ripple in the power supply to the author. Although not well known in the field of high power technology, the fluctuation of a potential of a floating power supply is ascribed to "the common mode" noise in the fields of electric, electronic circuits and microwave circuit[47]. The term "common" mode voltage appears to be loosely defined as a ripple voltage with respect to the ground. This common ripple potential, which is caused by the return current (I-J), is developed across the stray capacitance of the neutral point of the thyristor

bank. Although in the HIMAC, this potential is zero to the first order, the concept of the common mode voltage is extended as a difference voltage.

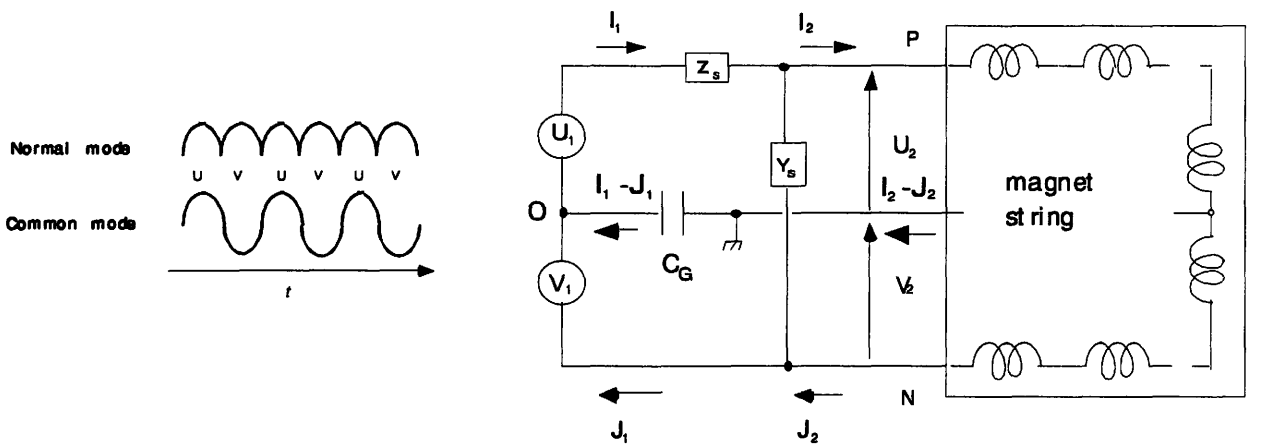

FIGURE 1. Model circuit of most of power supplies.
The voltage source is floated of which degree of isolation is given by the stray capacitance C_G at a neutral point O of the thyristor bank to the ground. U_1 and V_1 operate alternatively and produce common mode ripple voltage.

Common Mode Concept

We applied the idea of the common mode to the synchrotron power supply, for the first time in an explicit form. The common mode voltage is the difference between the voltage from the ground to the positive line designated as U_i in Figure1 and the voltage from the negative line to the ground designated as V_i, namely U_i-V_i where i=1 and 2 in the Figure. The common mode current is the one that flows through the ground line or the sum of the two outgoing currents directed towards the load, namely in either case designated as I_i-J_i. This current is equal to that of the difference current of outgoing current and incoming current. The normal mode voltage is defined as the sum of U_i and V_i, namely U_i+V_i. The normal mode current is the sum of the outgoing current to the load and the incoming current from the load and is expressed as I_i+J_i. The normal mode voltage is the one across the output of power supplies. The normal mode and the common mode make a complete set describing the electric property of the system.

Besides the mode concept we also applied the concept of the "symmetry" and the "decoupling" as a basic design rationale. The keyword "orthogonarity" instead of "decoupling" has been used in author's previous

literatures. Elements of the power supply system such as the reactor transformer, capacitor, magnets etc., are "symmetrically" located with respect to the ground line. The author found, with perfectly symmetric configuration, that this leads to the "decoupled" treatment of the normal and the common mode analysis of the power supply system [39,40].

One of the distinctive feature of the HIMAC synchrotron in reducing the ripple current is the common mode filter. In most of existing power supplies system the common mode low pass filter is not implemented. Without the common mode filter, the common mode ripple or abrupt change of voltage generated in the power supply, could pass through the low pass filter without being attenuated. There is a chance that this spike voltage is resonantly enhanced in the load of magnet strings as a current spike because of the resonant property of both the power supply and the load. Furthermore some existing low pass static filters, which are a normal mode filter, are asymmetrically configured with respect to the ground line; the reactor transformer is placed only one side of the power supply as shown in Figure1. The normal mode ripple could transform into the common mode ripple in asymmetric filter. In the equivalent circuit of these power supplies, the earth line is neglected and an outgoing current I_1 and the incoming current J_1 are assumed to be equal. In actual operation, the ripple or abrupt change of voltages U_1 and V_1 are alternatively generated and produce the common mode voltage besides the normal mode voltage. Due to its nature of alternative generation of the voltage of U_1 and V_1, the frequency of the common mode ripple is half of the frequency of the normal mode ripple voltage as shown in Figure 1.

In the HIMAC, an attention has been paid to realize a symmetry between the positive line and the negative line. There may be a violation of the symmetry due to the imperfection of the hardware. In existing synchrotron power supplies without conscious recognition of the common mode concept, a degree of asymmetry may be more conspicuous.

Mode Mixing

Asymmetric configuration causes the mode mixing between the normal mode and the common mode[37]. In presence of the mode mixing, the common mode voltage before the normal mode filter is transformed into the normal mode and vice versa. At the output of the normal mode filter, there is a chance that the magnitude of the normal mode ripple or the spike could

be larger than that of the case without mode mixing. In this way, in existing filters there may be cases that the normal mode ripple is not attenuated as expected. One of the causes of the performance limit in the output of the existing power supplies is explained by this common mode ripple whose amplitude is much greater than that of the normal mode at the input of the load.

With a perfect symmetric configuration where the reactors Z_s are at Positive(P) and Negative(N) lines in Figure1, the modes are decoupled and there is no mixing. Although the normal mode ripple is attenuated, the common mode is not attenuated and the ripple or abrupt change of voltage propagates down the filter to the magnet string. In either case of asymmetric or symmetric case of the existing configuration, the common mode plays a significant role in evaluating the ripple and the spike.

Grounding the Power Supply

In most power supplies, the neutral point O of the thyristor bank is isolated. The degree of isolation is measured by the capacitance C_G of Figure 1. The common mode current designated as I_2-J_2 returns from the magnet strings through the stray capacitance and drives the potential of the neutral point O oscillatory. The existence of the common mode current in the power supply also indicates the existence of the stray capacitance of the load as in the power supply. This current flows into the ground through the stray capacitance. By the energy conservation law this common mode current must return to the ripple voltage source, namely the neutral point of the thyristor when the system of the power supply is decoupled from other electrical systems.

In the HIMAC, we decided to ground the neutral point so that the normal mode filter and the common mode is symmetric. This grounding causes the common mode ripple and spike current to flow in the ground line and to return to the thyristor bank. This means the common mode noise increases in the ground line. This also means the noise is confined in the power supply system. Due to the common mode filter, the ripple and spike current does not flow in the magnet coil but is bypassed through the capacitor of the common mode low pass capacitor.

Ladder Circuit

In a design report of CPS at CERN, a magnet string was modeled as a

ladder circuit. This is a circuit of repeated elements of an inductance L of the magnet, a stray capacitance C between the coil and the yoke and resistance r of the excitation coil. We adopted this model in the HIMAC. There the upper coil runs toward the neighboring coil in series instead of connecting to its lower coil of the same magnet and again is connected to the separated upper coil of the next neighboring coil and so on. So does the lower coil. The connection of the upper and the lower coil is done at the end of the load. In existing magnet string, the upper coil is connected to the lower coil then go to the next neighboring coil. The magnet yoke is regarded to have ground potential and they are all connected in series by the earth line in the HIMAC. The basic model circuit is shown in Figure 2. The important consequence of this connection method is a symmetric property of the load with respect to the ground. The magnitude of the impedance between the common and the normal differs. This is due to the mutual coupling between the upper and lower coil. The magnet string is a repeated circuit of the unit cell of concentrated elements and is called a ladder circuit.

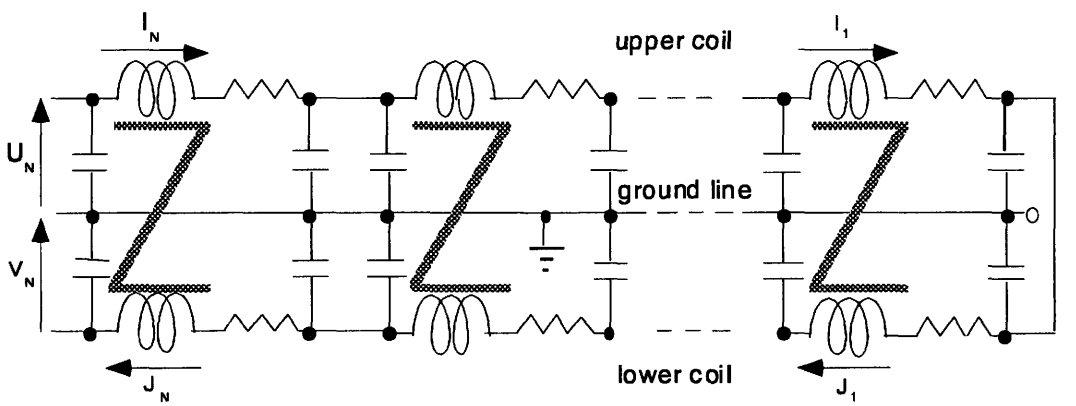

FIGURE 2. Magnet string modeled by a Ladder Circuit.

The upper coil and the lower coil are separately connected but magnetically coupled through iron yoke.This coupling results in a reduction of the common mode impedance and canceling effect of the magnetic field in the magnet gap.

Ladder circuit shows a similar property of a transmission line circuit below a certain frequency, which is around 100 kHz in the HIMAC, and has a feature of parallel and series resonances.The series resonances should be avoided as the admittance increases at the resonant frequency. In the report by Regenstreif[19] only the normal mode component is analyzed. They did not refer to the common mode. Examination of the ladder circuit of Figure2 reveals the existence of the common mode. Researchers thereafter did not

pay attention to this configuration since then except S. Van der Meer[20]. He pointed out that the synchrotron magnet string behaves as a transmission line and the sudden change of magnet voltage excites standing waves and the transient current is excited. The bridge resistor is introduced to damp the resonance. They evaluated the bridge resistor connected in parallel to the coil to reduce a closed orbit distortion. They did not refer to the relation between the earth of the power supply and the earth of the magnet string which plays a key role in reducing the ripple.

The common mode impedance is introduced by R. Schafer [21,22,23,24] in a transmission line model of Tevatron and SSC and by others [25,26,27,28]. It was pointed out by the author that the common mode is a major source of ripple and spike in previous synchrotron power supply system. Taking measures against the common mode have not been done explicitly until now by any other authors. Part of our formulation of the mode analysis, performance and design principle has been already published in several conferences [29,30,31]. In this article a characteristic feature of the HIMAC power supply and the performance are described.

II. Symmetry and Mode Decoupling

The "symmetry" and the "mode decoupling" is adopted as the underlying principle of our design of a synchrotron power supply. By a property of the "symmetry", where equations remain unchanged when exchanging relevant parameters, two modes of the normal and the common are treated by a unified equation. Property of the "mode separation" assures an independent handling of parameters, avoiding a complicated system of coupled parameters. To assure the "mode separation", we have tried to make a geometric symmetry in the elements of the power supply and the load as shown in Figure 3. Here ground line is taken as a reference to the P line and the N line. With the exception of the firing sequence of the thyristor bank, the LCR elements, the voltage and current sensors for diagnostics, and filters are all placed symmetrically with respect to a ground line. The neutral point O of the four stage thyristor blocks and all iron yokes of the load are connected and grounded to the earth. Thyristor and the ladder circuit load are connected and the ground potential is maintained by a single common earth point. A common mode static filter as well as a normal mode static filter is employed and are providing the suppression of the thyristor spike of

both modes. The capacitor of the common mode static filter is connected to the earth line of the thyristor and the load, providing a single earth system. Although it is omitted in Figure 3 and shown later in Figure 15, the reactor transformer of the active filter is connected in symmetrical way. By a symmetrical placement of similar elements, a separate treatment of the normal and common mode is possible. To the best of the author's knowledge, the earthing of the mid-point is employed in LEP[2] and the symmetric placement of the elements is in LEP[2] and synchrotron light source at ANL[47].

To realize a symmetry of firing the thyristor means an increase in the number of thyristors by factor two, although it has merit in suppressing the common mode voltage. Increase in the number of thyristors leads to increase in a cost. Error in the timings of simultaneous on-off leads to a development of a common mode ripple and spike. We chose to set up the common mode filter rather than increasing number of thyristors.

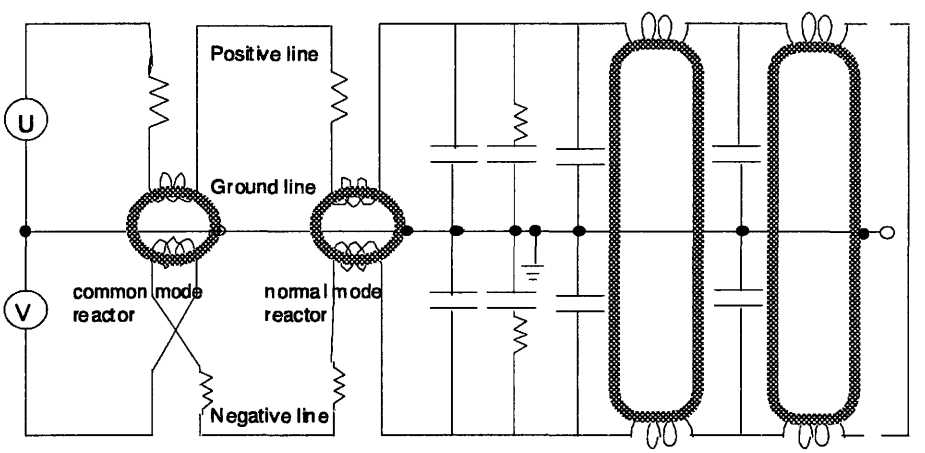

FIGURE 3. Symmetric Circuit of the HIMAC Power Supply and Load.
The normal mode and common mode reactor, capacitor to the ground, upper and lower coils are placed symmetrically with respect to the ground line.

Due to the symmetry, we can decouple the modes and attenuate, both the ripple and the spike by the symmetric mode filter. Furthermore, there is a way to considerably reduce the effect of the common mode in a form of a magnetic field. This is done by devising the way of a separate connection of the excitation as described in the next section.

III. Separate Connection of Coils and the Ground Line

To realize higher symmetric configuration, the magnet coils are divided into two parts; namely the upper and the lower coils. Furthermore, the ground line was set to run along the P and N cables to assure the ground potential of reference. All the upper coils are connected together in series. All the lower coils are connected in the same way. Both coils are connected at the end of the magnet string.

Outstanding effect of this symmetric connection is its canceling effect of the magnetic field due to the common mode current. Suppose an outgoing current is I_n and incoming current is J_n, then, the current of the upper coil I_n and the current of the lower coil J_n are written as,

$$I_n = \frac{I_n + J_n}{2} + \frac{I_n - J_n}{2}, \qquad J_n = \frac{I_n + J_n}{2} - \frac{I_n - J_n}{2}.$$

Each current is expressed as a linear combination of the normal and the common modes. Sign of the normal mode current is opposite of that of the common mode current, or in other way, the normal mode current is a anti-parallel current and the common mode current is a parallel current. Figure 4 schematically depicts how the magnetic field in the gap is generated by the common mode current of the HIMAC Bending magnet and Quadrupole magnet. In the Bending magnet, the common mode current of the upper coil and the lower coils generates the field of opposite direction. The common mode inductance in this case is nearly zero. In the Quadrupole magnet, the magnetic field on a horizontal plane is canceled out but not on the vertical plane as illustrated in the right of Figure 4.

In most of synchrotrons, the upper and the lower coil are not separately connected and a common mode filter has not been installed. Current ripple and current spike appear as a mixed mode without being attenuated in the load. Though the common mode ripple and spike do not directly appear as a magnetic field on a horizontal plane, it is safer to suppress the common mode as it may appear as a normal mode due to the mode mixing. As an asymmetry arises either by an unbalance of the capacitance of the impedance. In particular, the spacing between the coil and the magnet yoke is small. Controlling this spacing is not easy. There may be a considerable fluctuation of the capacitor to the ground.

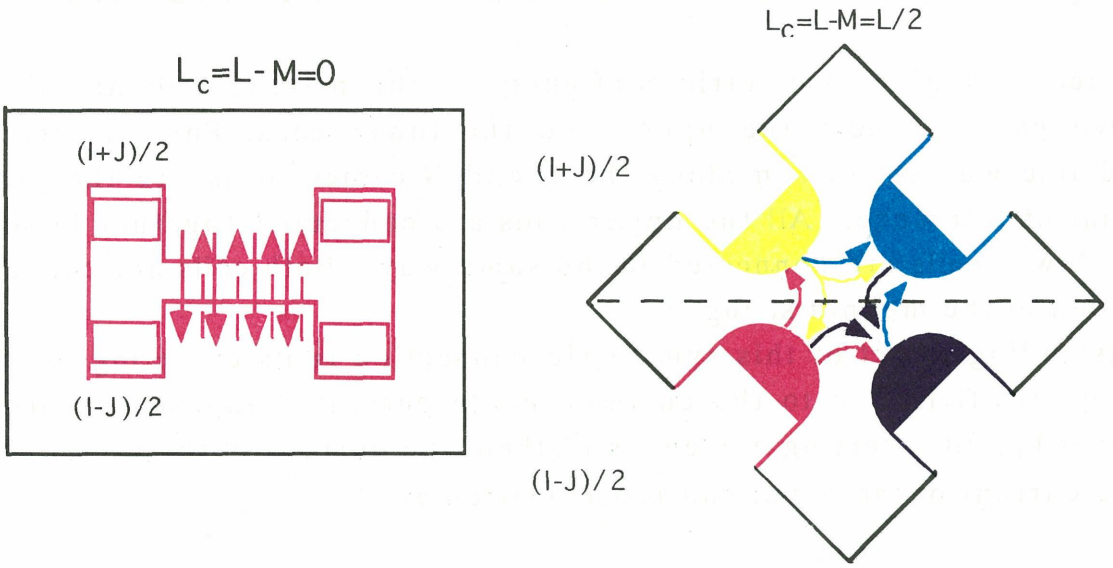

FIGURE 4. Canceling effect of the magnetic field due to the common mode current in Bending magnet(left) and Quadrupole magnet(right) at the HIMAC.

Although being indirect, there was an effort to reduce the common mode spike by trying to reduce a stray capacitance to the ground of the power supply[16]. As a thyristor spike frequency is inherently high, reduction in magnet's capacitance results in a further increase of the spike frequency and sufficient amount of suppression is not realized. It should be noted the reduction of a capacitance to the ground brings in an increase of the impedance of the return path of the common mode spike to the thyristor. The common mode spike being blocked to return has to find its way back through a route of lower impedance, and this results in a radiation of the ignition spike noise to the outside environment.

On the other hand, the neutral point of the thyristors is grounded in the HIMAC. The low impedance of the return path results in a suppression of a radiation of the common mode spike noise to the outside environment. In this way, the high frequency spike noise from the thyristor power supply is suppressed to a level of a negligible amount.

Earth line can also be used as a reference potential of an electronic logic circuit. It is expected even when the potential of the neutral point oscillates, the potential of the low level circuit simultaneously oscillates with it, and the difference in the potential between them is kept small. HIMAC's high performance of the active filter owes to this property.

IV. Symmetric Mode Filter and its Performance

HIMAC low pass mode filter consists of a normal and a common mode filter. Each filter consists of the series reactors and the parallel capacitors. The capacitors are placed between the P line and the earth line, and between the N line and the earth line. Performance of the low pass filter is measured by the four channel FFT analyzer of Hewlett Packard with power amplifier and the Fluke's shunt resistor. Configuration to measure the admittance of the magnet string is shown later in Figure 9.

Spike and ripple, except the low frequency illogical ripples of 50 Hz and 100 Hz, are considerably suppressed by the symmetric low pass filter. Figure 5 shows a simple block diagram of the simplified model of the symmetric mode filter. Z_s represents the normal mode reactor and the common mode reactor. Y_a represents the capacitor to the ground.This capacitor is used for the common mode and the normal mode. Y_1 is usually neglected in existing models.

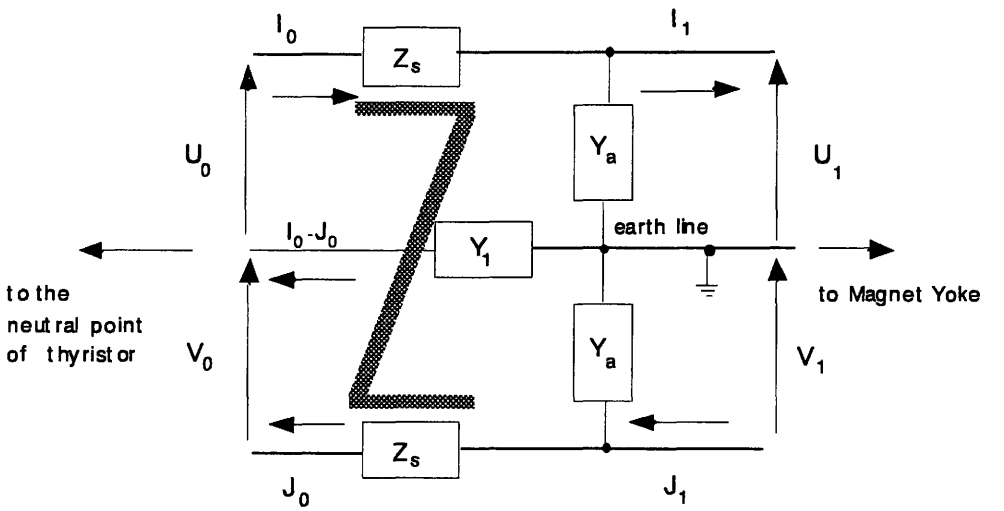

FIGURE 5. Simplified block diagram of the symmetric filter of the normal and the common mode. Z_s is a reactor transformer.

Filter terminated with Infinite Impedance

In order to understand a feature of the symmetric mode filter, let us simplify the model such that the ripple voltage at the input is given and the impedance of the load is infinitely high. The ratio of the output voltages of the filter and those of the each thyristor bank for both mode, G_n and G_c, can

be derived as,

$$G_n = \frac{U_1 + V_1}{U_0 + V_0} = \frac{1}{1 + (Z_s + Z_M)Y_a} \tag{4-1}$$

$$G_c = \frac{U_1 - V_1}{U_0 - V_0} = \frac{1}{1 + 2\frac{Y_a}{Y_1} + (Z_s - Z_M)Y_a} \tag{4-2}$$

where Z_M is the mutual impedance and Z_s is the self impedance of the reactor transformer of the low pass filter. The reactor transformer is made of the normal mode reactor and common mode reactor such that the sign of the mutual inductance is out of phase, namely $Z_s = sL_s$ for the normal mode reactor, and $Z_s = -sL_s$ for the common mode reactor. Z_M is not necessarily to be finite in constructing the common mode filter.

The admittance Y_a is composed of two capacitance C_{a1}, C_{a2} and a resistance r_{a2} so that the slope of the decay with increasing frequency is sharper, at the cost of a slight increasing the magnitude of the transfer function as proposed by Praeg[15],

$$Y_a = sC_{a1} + \frac{1}{\frac{1}{sC_{a2}} + r_{a2}}. \tag{4-3}$$

Ratio of C_{a2} to C_{a1} is chosen to be 5 and r_{a2} is 1 Ω and the magnitude of the transfer function slightly increases below the cut-off frequency. In the HIMAC, the neutral point of the four stage thyristor block is grounded and hence the second term in the denominator of the eq.(2) is zero and the common mode transfer function of the voltage is ,

$$G_c = \frac{1}{1 + (Z_s - Z_M)Y_a} \tag{4-4}$$

which is the same form of the transfer function of the normal mode except for the sign of Z_M. In an existing configuration, where the neutral point of the thyristor bank is not grounded and the capacitance to the ground is not implemented, Y_1 and Y_a in eq.(4-2) could be interpreted as a stray capacitances to the ground. The Z_s may also be a self inductance of a cable or a bus bar. In this case eq.(4-2) is reduced to

$$G_c \sim 2\frac{Y_1}{Y_a}. \tag{4-5}$$

Thus in existing power supplies, the magnitude of the stray capacitance to the ground needs to be smaller than that of the stray capacitance to the

ground from the bus bar, otherwise there is a possibility that the ripple or spike may be enhanced. The normal mode and common mode filters are made to be identically. Figure 6 show the calculated frequency dependence of the low pass filter. The relevant parameters for the case of the HIMAC are,

$$L_s = 1 \text{ mH}, \; C_{a1} = 1 \text{ mF}, \; C_{a2} = 5 \text{ mF} \text{ and}$$

$$r_2 = 2\sqrt{\frac{L_s}{C_{a2}}} = 0.894, \quad f_1 = \frac{1}{2\pi\sqrt{L_s C_{a1}}} = 159.19, \quad f_2 = \frac{1}{2\pi\sqrt{L_s C_{a2}}} = 71.178.$$

There is a small peak in magnitude in the transfer function of the low pass filter at the frequency of f_1=71 Hz as seen in Figure6. The peak occurs either at the frequency of f_1 or f_2 which both depend upon the magnitude of the resistor r_2. Measured frequency dependence of the transfer function of the normal mode and that of the common mode filter are shown in Figure6. Although the performance is rather satisfactory, deviation of the magnitude of the transfer function from the simple model described above is observed around frequency of several kHz. Deviation of the phase starts much earlier, below 1 kHz. Furthermore the performance of the common mode filter is better than that of the normal mode filter. The deviation and the difference between the two filters may be partly explained by the difference in the quality of the reactor transformer where the deviation of the inductance is observed around several kHz.

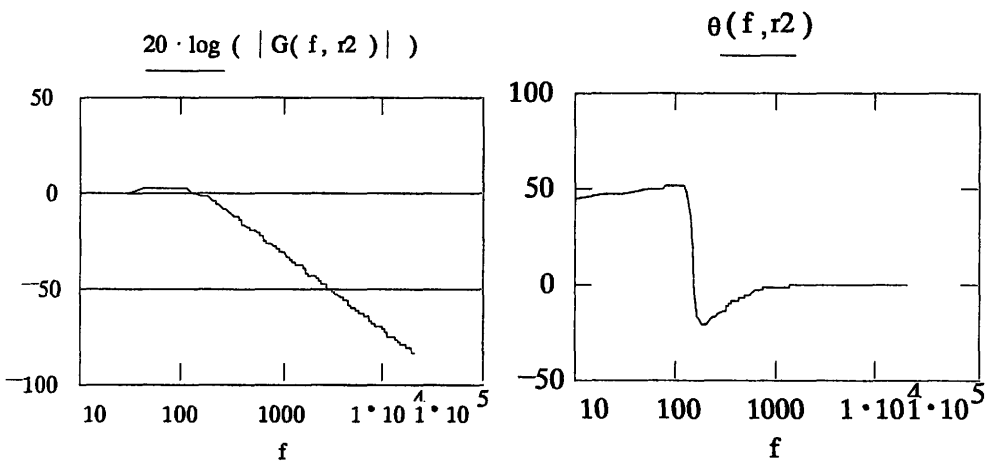

FIGURE 6. Frequency dependence of the magnitude and the phase of the transfer function $G_{n,c}$ of the Low pass mode filter (calculated).

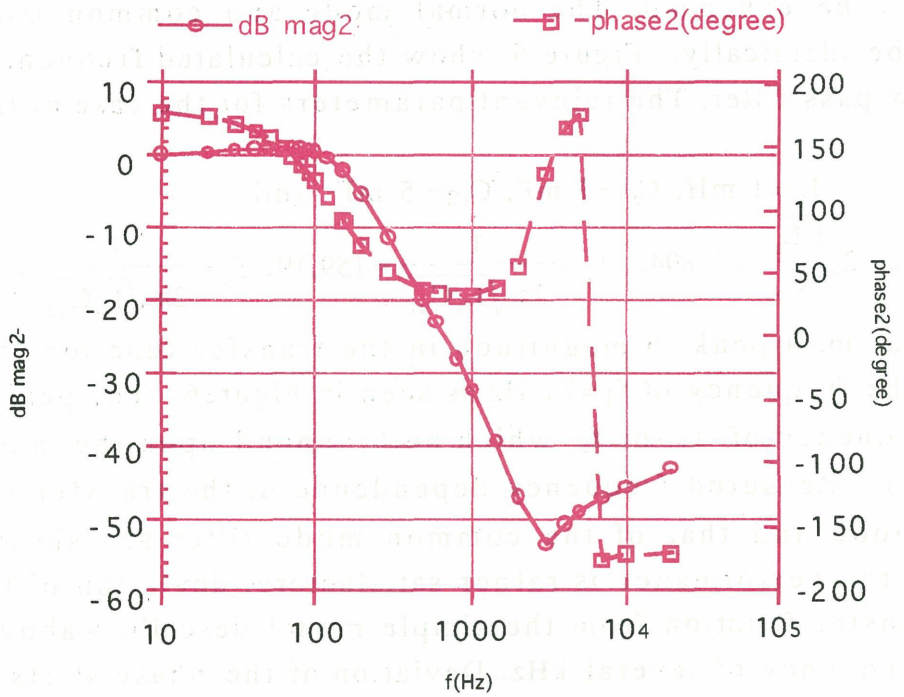

FIGURE 7. Frequency characteristics of the normal mode low pass filter transfer function G_n (Quadrupole). Deviation is seen above several kHz.

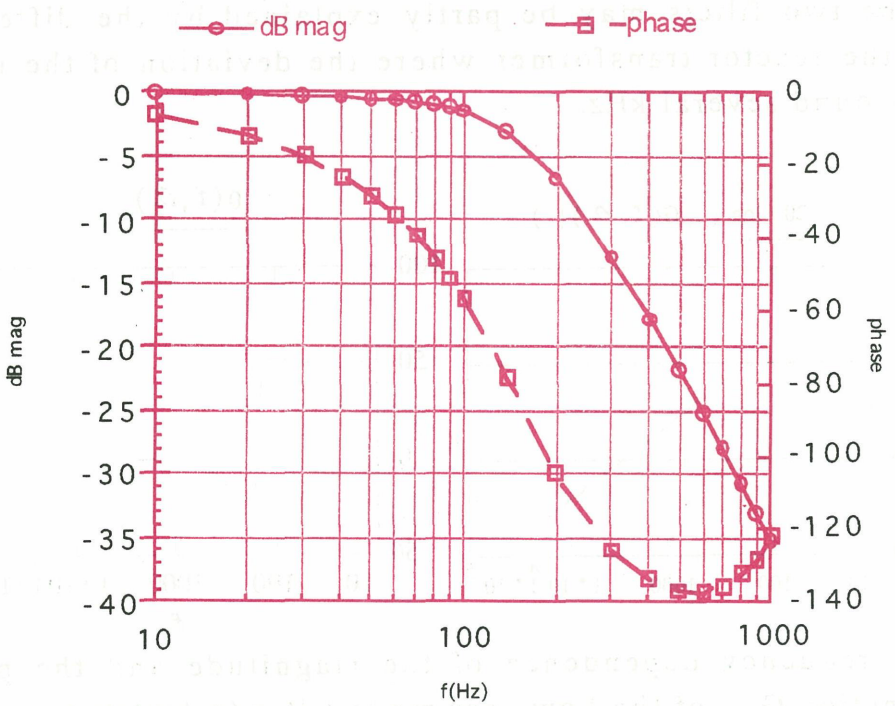

FIGURE 8. Frequency characteristics of the common mode low pass filter transfer function G_c (Quadrupole). Deviation from the calculation is observed above 6 kHz.

V. Summary of Mode Analysis of a Ladder Circuit

We will make a short summary of the mode analysis of the ladder circuit of a HIMAC synchrotron power supply and its load[39]. The excitation coils are divided into upper and lower coils for the dipole magnet. For a Quadrupole magnet, there are several ways to separate them out into two parts. In the case of the HIMAC Quadrupole, upper and lower coils are grouped from the view point of a simple connection. It is possible to group the coils of the North and South poles, where in this case, physical connection is more complicated but the reduction of the common mode inductance is expected as much as the Bending magnet.

A single magnet with stray capacitances may be represented by a six terminal circuit of three inputs and three outputs. For an ease of analysis, this unit cell is treated as "symmetric" for interchange of the input and the output. Voltages across the earth and P, and N lines of the power supply is designated as U and V respectively with a suffix. Currents flowing in the P and N lines are designated as I and J. Elements of "symmetric " nature such as the magnet, a reactor and capacitance with respect to the earth line leads to a separation of a coupled mode into a decoupled mode. Where the normal mode is designated as $(U_n + V_n)$ and $(I_n + J_n)$ and the common mode is designated as $(U_n - V_n)$ and $(I_n - J_n)$. Although mathematically, the mode separation is possible by finding an eigenvalue and an eigen vector in the case of an "asymmetric " circuit with respect to the earth, a symmetric circuit is much easier to handle and to find a way to suppress the harmful spike and ripple.

Mode separation enables us to convert the six terminal circuits into well known four terminal circuit[39]. A relation of the input and the output voltages and those of the currents are expressed by two by two transfer matrices for the decoupled four terminal circuit whereas they are expressed as four by four transfer matrices for the six terminal ladder circuits. The corresponding second order differential equations are unified and have the form of transmission equation.

Following our design principle of the "symmetry" and the "mode separation", or "orthogonality", we chose an open-ended condition for the common mode circuit, where the furthest end of the ground line is left open. The end of the normal mode circuit where the main excitation current of the magnet flows, is shorted. Imposing these terminal conditions to each

equivalent circuit, we obtain a set of solutions, where two mode are independent each other, for the normal and common mode. For the common mode, the choice of termination with a characteristic impedance is possible. We preferred to take "orthogonal" property of the function rather than impedance matching. In the case of impedance matching, it is necessary to find the stray capacitance of the load experimentally.

The admittance of the normal and common modes of the ladder circuit is expressed by a product of the characteristic admittance Y_{op} which is the inverse of the characteristic impedances Z_{op}, where for the normal mode p=n and for the common mode p=c, and a hyperbolic sinusoidal function,

$$\mathcal{Y}_n = Y_{on}\coth(N\varsigma_{mn}) \tag{5-1}$$

$$\mathcal{Y}_n = Y_{oc}\tanh(N\varsigma_{mc}) \tag{5-2}$$

where N is the number of cells and ζ_{mp} is the phase advance per cell and is expressed as,

$$\cosh(\zeta_{mp}) \equiv 1 + Z_{mp}Y_{mp} \tag{5-3}$$

$$Y_{op} = \left[\frac{Z_{mp}}{(2+Z_{mp}Y_{mp})Y_{mp}}\right]^{-\frac{1}{2}} \tag{5-4}$$

where Z_{mp}, Y_{mp}, are the impedance and the admittance of the normal and common mode of the unit cell. The characteristic impedance of the admittance given by the eqs.(5-4) slightly differ from those of the transmission line. The equations show that at the output of the power supply or at the input of the ladder circuit, there exists N parallel and series resonances. The amplitude of the admittance at the resonant frequency depends upon the magnitude of the resistance in parallel to the inductance. The resonance of the lowest frequency appears as a parallel resonance for the normal mode admittance, and as a series resonance for the common mode admittance. In many existing synchrotrons, where the impedance of the common and the normal mode is identical, the first series resonance of the lowest frequency appears as the common mode. Therefore, beside the fact that they do not have a common low pass filter, the common mode resonance rather than a normal mode resonance is more problem.

The admittance of the HIMAC ladder circuit is measured by applying the swept output voltage of the Hewlett Packard's digital FFT analyzer, HP35670A, to the load as shown in Figure10. The voltages of U, V and the currents I and J are monitored simultaneously. The sum, difference and division of these parameters are done by using the mathematical function of the FFT analyzer. From a comparison of the measurement of the admittance of the actual load with the calculation, it is better to introduce a resistor of several kΩ in parallel with the excitation coil in the model to have better fitting. This resistance is interpreted as an equivalent loss of the magnet. With this parallel resistor, the amplitude of the resonance of lower frequency is more damped than that of higher frequency.
In Figure10, typical voltage spectrum of the normal and the common mode ripple voltage are shown. One can see 1200 Hz is the major ripple frequency for the normal mode and 600 Hz for the common mode. In Figure11, the calculated admittance of the Quadrupole is shown. As the frequency increases, the resonance is gradually damped and approaches a constant value. This constant value is the characteristic impedance of the ladder circuit. Due to this saturation-like property, the admittance of the magnet string is roughly constant at higher frequency. The admittance measured in small signal excitation using FFT analyzer is shown for comparison in Figure12. The observation and the theory agrees.

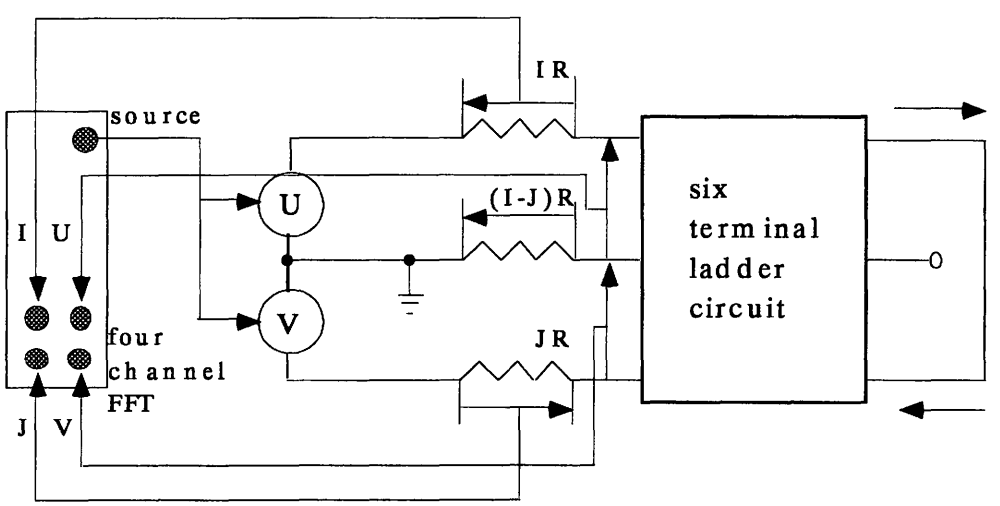

FIGURE 9. Measuring circuit of the admittance by four channel FFT analyzer. Swept voltages from the source output of the FFT analyzer are applied to the ladder circuit. The amplitude of the voltages U and V are set to be different by the attenuater, so that the net common mode voltage U-V is finite.

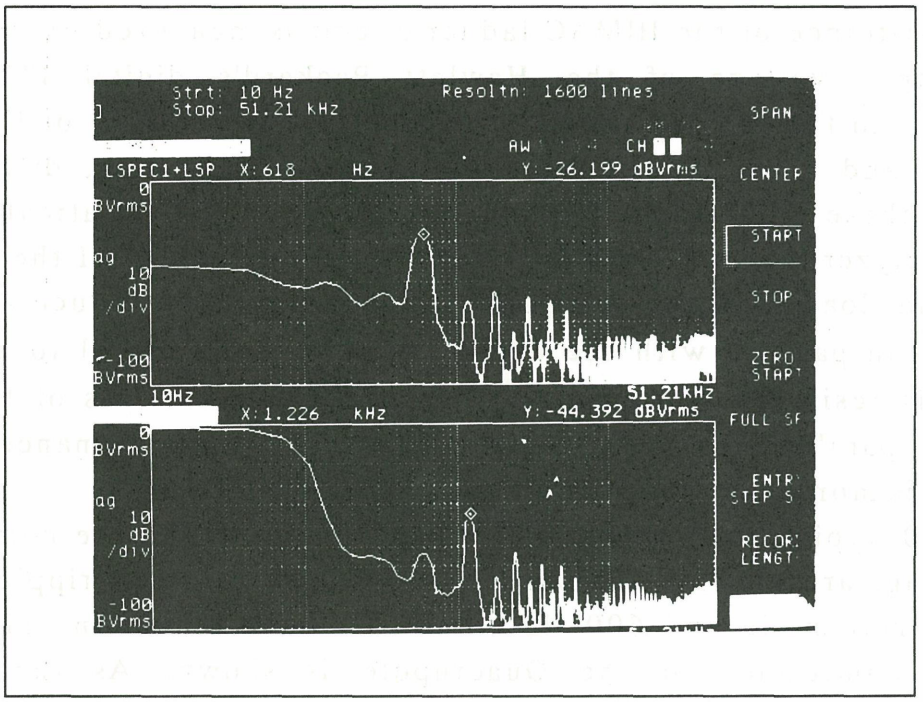

FIGURE 10. Typical ripple voltage specrum of the common mode(upper trace) and the normal mode(lower trace). The fundamental frequency of the normal mode is 1200Hz and that of the common mdoe is 600 Hz. Horizontal axis is 10 Hz to 51.21 kHz.

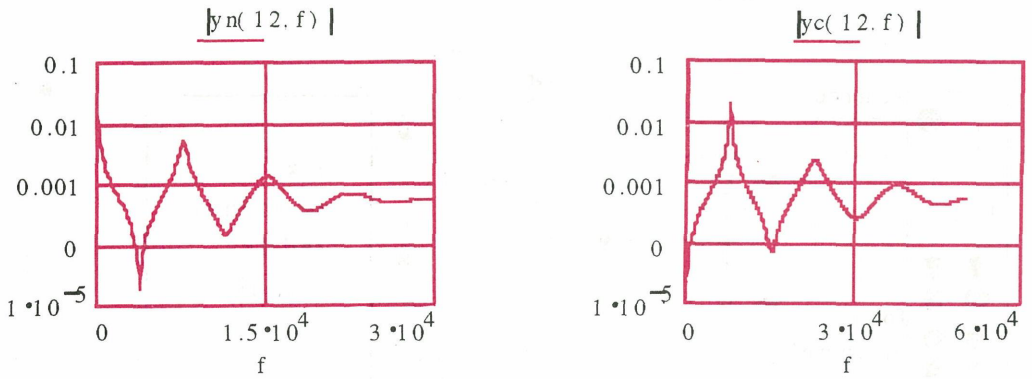

FIGURE 11. Normal mode(left) and common mode(right) admittance of Quadrupole magnet without bridge resistor(calculated). The effective resistor of 6 kΩ is taken into account.

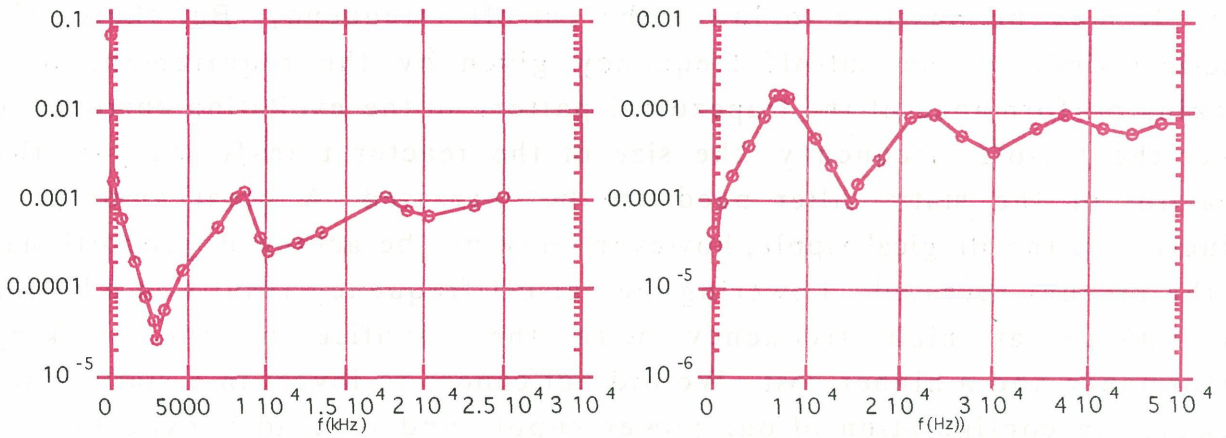

FIGURE 12. Normal mode and common mode admittance of the Quadrupole magnet without bridge resistor (unit in Ω^{-1}, Measured).

With an installment of a bridge resistor, 20 Ω for quadrupole and 100 Ω for the dipole, in parallel to the coil, the resonance is shown to be completely damped. The magnitude of the bridge resistor is chosen to be less than the one required to damp the resonance. This is because the bridge resistor has an additional role of bypassing the logical ripple as well as damping the resonance of a thyristor spike. The observation of the output of the one turn coil of yokes of a quadrupole magnet shows a reduction in the amplitude of the fundamental logical ripple of 1.2 kHz as shown later in Figure 18. The bridge resistor also helps to damp the reflected wave of the current spike.

Idea of symmetry and mode separation lead to the construction of the common mode filter. With a common mode filter, logical harmonic ripple and spikes are suppressed. For the case of a Bending magnet power supply, 5 ppm is achieved by low pass filter even in the absence of the active filter. For the case of Focussing Quadrupole magnet power supply, we have to attenuate the illogical ripples. The mode filter alone is not enough and the active filter is used as described in the next chapter.

VI. Suppression of Illogical Ripple

Thyristor spikes and high frequency logical ripples are suppressed by the method discussed in previous chapters. However, the illogical ripples such as 50 Hz and 100 Hz cannot be suppressed either by the normal or a common mode static filter because the cut-off frequency is at 71 Hz in the HIMAC. Magnitude of the 100 Hz ripple is even enhanced in the Praeg type

filter. It may be possible to lower the cut-off frequency. But there is a practical limit of the cut-off frequency given by the requirement of a tracking performance of the trapezoidal pattern of the excitation current. To lower the cut-off frequency, the size of the reactor transformer or the capacitor of the static filter needs to be increased. A great amount of reduction in the illogical ripple, however, may not be achieved, proportional to the amount invested. Lowering the cut-off frequency results in a better performance at high frequency with the sacrifice of the tracking performance and a higher cost. We did not choose to invest in a static filter because the configuration of our power supply and its load is expected to show excellent high frequency characteristics without lowering the cut-off frequency.

With an introduction of a systematic earthing system in the HIMAC power supply and its load, a control system can operate in a quiet environment in spite of the operation of a high power thyristor system.The block diagram of the control system of the power supply system is depicted in Figure 13. The control system consists of the active filter, ACR (Automatic Current Regulator), mAVR (minor Automatic Voltage Regulator) and a digital repetitive control system. The active filter is located "symmetrically" at the P and N lines and power is fed by mutual inductance into a seriesly connected reactor transformer. The input of the active filter is the voltage from the output of the low pass filter, the voltage V_c from the CPU and the output from ACR.

The common and normal mode voltages are sensed and fed into the upper and lower reactor transformer through the high pass filter. High pass filter is placed to cut the DC and slow component and to pick up the ripple and transient component after the smoothing section in the flat top pattern. The transfer function of the high pass filter is set as,

$$\frac{s^2}{s^2 + 2\xi\omega_c s + \omega_c{}^2}$$

where ω_c is 100 rad/s for $\xi = 1$ for Quadrupole power supply and 14 rad/s and $\xi = 1/\sqrt{2}$ for later installed Bending Magnet power supply.To compromise the performance of the tracking of the pattern and the performance. ω_c and ξ are adjusted. The input of the ACR and the digital repetitive control system is a DCCT which is located at the furthest end from the power supply side. A frequency of the major ripple content of the DCCT is 50 Hz and its relative

magnitude at full rating is as low as 60 ppm. Fortunately the frequency of other ripples was much smaller than 50 Hz ripple.

In spite of the non-negligible 50 Hz ripple in the DCCT, which is 50 ppm, we have achieved a reduction of the relative ripple content in the output of the power supply, by two orders of magnitude less than that of the DCCT. This is done by inserting a low pass analog and digital filter with a cut-off frequency of 25 Hz. The analog low pass filter is placed between the output of ACR and the input of the high pass filter of the active filter. The digital filter is placed in the digital repetitive control loop which is not shown in Figure 13.

Beside the control system mentioned above, we have developed and installed various devices containing high performance. Due to a high performance of the SVC (Static Var Controller)[32] using a thyristor controlled reactor and an algorithm of a learning system, the stability of the voltage from the primary line is maintained precisely, and any imbalances are adjusted at a level of 0.1 %. By using PLL (Phase Locked Loop)[33] an equalization of the firing timing of the thyristor is set within an accuracy of a several μsec.

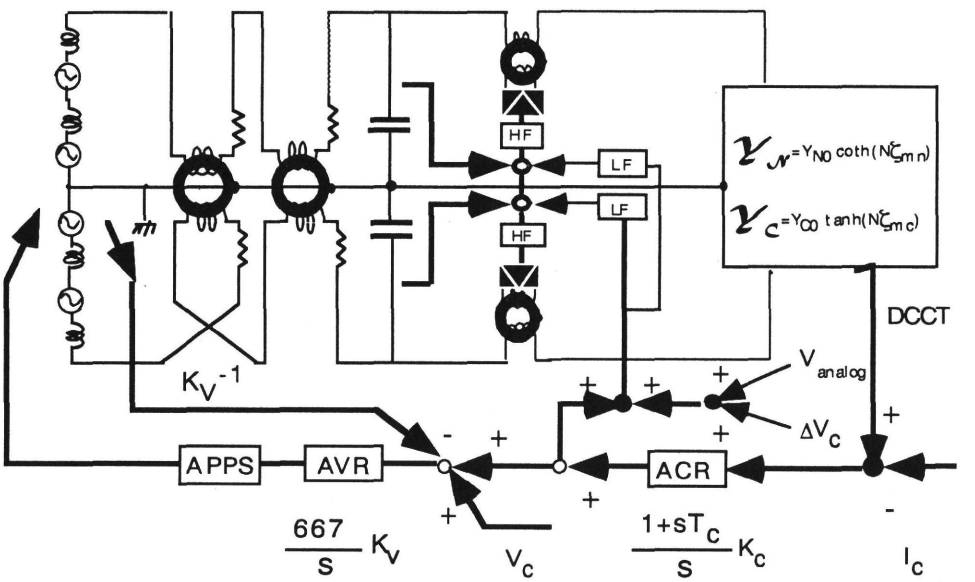

FIGURE 13. Block diagram of the control circuit.
The control circuit consist of minor AVR, ACR, APPS, Active Filter and Digital Repetitive control. LF denotes the low pass filter. K_c is 52 and $T_c=44/K_c$.

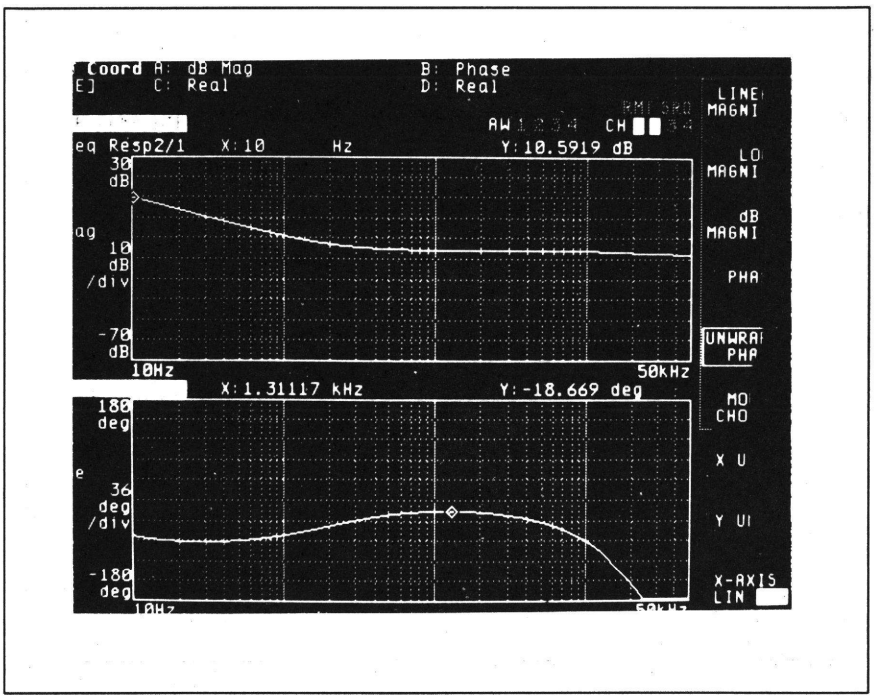

FIGURE 14. Frequency response of the High pass filter of the Active Filter

VII. Ripple Performance

Performance of a power supply system is measured by relative ripple content of the output current normalized by a rated current. The accuracy of the current measurement at the ppm level is not available at present technology. We are currently developing to detect the ripple current below ppm level by measuring the bypassed current of the bridge resistor and it is promising[42]. The accuracy of the NMR may be close to this accuracy but the NMR is only applicable to DC or slow time varying field. NMR is only applicable to a homogeneous field with a condition that the magnetic field is kept constant during the period of at least 10 msec. It is said the beam spill is the best detector of the ripple of the power supply. This is because of the tight requirement of the ripple content during the slow extraction. However, the qualitative relation between the beam spill and the ripple content is not yet known neither from the theory nor the experiment. At present we are also working to find this relation from the experiment.

We have evaluated the current ripple by calculating from the measured voltage and the measured admittance of the magnet string. The admittance is measured from by exciting the magnet string with low level signal using

the digital FFT analyzer and the power amplifier. The ripple voltage is measured at the location after the low pass filter. The dividing ratio of the resistor is 1 to 50 for the Quadrupole magnet power supply and 1 to 300 for the Bending magnet power supply. For the Quadrupole, -60 dBV of ripple voltage corresponds to roughly 0.8 ppm in relative current for 1000A of 100 Hz. The maximum current of the Quadrupole is 1350A and 2260 A for the Bending magnet. Thus, the relative ripple amplitude of the ripple voltage $x(dBV_{rms})$ for the Quadrupole, the relative ripple current $\delta(x)$ is written as,

$$\delta_n(x) = q\frac{10^{-\frac{x}{20}}}{I_{max}} Y_{0n}\coth\left(N\zeta_{mn}\right) \tag{7-1}$$

$$\delta_c(x) = q\frac{10^{-\frac{x}{20}}}{I_{max}} Y_{0c}\tanh\left(N\zeta_{mc}\right) \tag{7-2}$$

where q=50 for Quadrupole magnet and 300 for the Bending magnet power supply.

For the Quadrupole, -60 dBV of the ripple voltage corresponds to roughly 0.8 ppm in relative current for 1000A. The maximum current of the Quadrupole is 2260 A and 1350 A for the Bending magnet. To measure the normal and the common mode simultaneously, four channel FFT was used. The magnitude of the ripple voltage is evaluated at the output of the power supply. An evaluation of the distribution of the ripple along the magnet string is not necessarily required in the HIMAC as the resonance is suppressed by the bridge resistor. However in a existing magnet where the resonance is not suppressed, the thyristor spike shows a sinusoidal distribution following the resonance. The bridge resistor bypasses the logical ripple and thyristor spike. This effect has to be taken into account. This is checked by measuring the induced voltage wound around yokes of the magnet. The accuracy of the measurement of the one-turn coil is not accurate as the ripple voltage from the resistor.

In next chapter, we first make a rough estimation on the ripple content on how much of the ripple content is required to allow for a third order resonant extraction.

VII-1. Requirement from Third Order Resonant Extraction

HIMAC consists of two identical ion synchrotrons with a single injector. They are operated out of phase so that the intensity of the total beam, as well as a total power of the power supply is as constant as possible. An injection energy of the beam is 6 MeV/u ($B\rho$=0.370 Tm). Maximum energy of the upper ring is 600 MeV/u ($B\rho$=4.246 Tm) and that of the lower ring is 800 MeV/u ($B\rho$=5.098 Tm). The extraction energy varies from 230 MeV to 800 MeV. Most of the operation energy is 290 MeV/u of which the amplitude of the excitation current is about 1/2 of a full current.

A circulating beam is extracted horizontally by a third order resonant extraction. To have a uniform beam spill, the rate of change of the area of a separatrix is required to be less than the specified value. For a horizontally extracted beam, the ripple content of a Focussing Quadrupole is more stringent than that of Defocussing Quadrupole by a factor of the ratio between horizontal and vertical betatron amplitudes, which is roughly 10.

Rate of change in the separatrix must not change exceed the width of the stopband during an extraction period Δt. This condition is written as,

$$\varepsilon_r(\omega) \leq \frac{1}{F\omega}\frac{\Delta Q}{\Delta t}$$

where F is the ratio of a change of a tune to that of a current , which is 5 in HIMAC, $\varepsilon_r(\omega)$ is a relative amplitude of the ripple with an angular frequency ω and $\Delta Q/\Delta t$ is the rate of change of betatron tune during extraction. In the above evaluation the stopband width is taken as 0.003 that is a measured value at the HIMAC. Generally the stopband width of the higher order is narrower than that of the lower order. Typical stopband width for a half integer resonance is 0.05. In case of the HIMAC, for ripples of 50 Hz and 100 Hz, $\varepsilon(\omega)$ must be less than 2.6 ppm(rms) and 1 ppm(rms) for 0.5 second of spill period respectively. This evaluation need to be confirmed by more accurate theory or experimental observation. In the GSI, the measurement of the relation between the ripple current and the beam spill is performed by introducing external ripple source of slightly different frequency into the power supply. At the HIMAC, quantitative evaluation between the ripple current and the spill is under study.

VII-2. Ripple Content of Focussing Quadrupole

A measurement of the current is not as accurate as that of the voltage Therefore, the ripple content of the current is estimated from a voltage measurement of the load by multiplying by the admittance. The admittance of the ladder circuit is not just proportional to the inverse of the frequency at higher frequency. The admittance or the impedance is calculated by the model proposed and can be measured by an FFT analyzer. Voltage ripple of the normal and the common mode was already shown Figure10 which was obtained during a process of improvement. Excitation current corresponds to an ion energy of 290 MeV/u. The thyristor spike was not observed. It is confirmed that the magnitude of the ripple does not change appreciably when the current is increased up to its maximum rating. The inductance and resistance of the load are 0.111 H and 0.117 Ω for the Quadrupole magnet and 0.633 H and 0.200 Ω for the Bending magnet.

Largest logical ripple is at fundamental frequency of a 24 pulse thyristor, namely, 1200 Hz of the normal mode. The second harmonic is much less, by 20 dB. Noting that the divider ratio of a breeder resistor is 50, one could roughly estimate the relative ripple content of 1200 Hz is 0.6 ppm (rms) at an energy of 290 MeV. This is equivalent to 0.27 ppm at full rating.
The relative ripple current in the excitation the cable using eq.(7-1) from Figure 16 is;

50Hz	-78 dBV	0.1 ppm	75 Hz	-73 dBV	0.1ppm,
100 Hz	-78 dBV	0.1 ppm	300 Hz	-65 dBV	0.1 ppm
1200 Hz	-44 dBV	0.3 ppm			

In the above frequency range, The admittance of the ladder circuit can be replaced by simple admittance of 1/(N(sL+r)). Due to the bridge resistor, magnitude of the coil current is smaller than the cable current. Furthermore the ripple of the actual current flowing in an excitation coil is reduced by the bridge resistor.

The dominant illogical ripples appearing in the Figure are 50Hz, 75 Hz, 100 Hz, 200 Hz and 600Hz. In an initial stage of a commissioning of the power supply, the 50 Hz and 100 Hz ripples were more predominant and the beam spill was plagued by them, although the harmonics except 50 Hz and 100 Hz were negligibly small. To suppress the illogical ripple, we have developed a Phase Locked external signal generator "Ripple Basher" whose amplitude and phase are adjustable manually. By adding it into the mAVR

voltage loop as an open-loop, almost every residual ripples are removed. Considerable amounts of improvement in the suppression of the 50 Hz ripple in the beam spill was not done though at an initial stage. By changing the cut-off frequency of a lowpass filter to 25 Hz, these illogical ripples were considerably reduced. The author found out that a source of the 50 Hz ripple has been generated in the control circuit itself. Further improvement was realized by using a bandpass filter of 50 Hz and 100 Hz and also by separating the power supply of the control circuit in the active filter. The 50 Hz and 100 Hz voltage ripple were selectively enhanced and fed to the power amplifier of the Active filter. Figure 15 shows a frequency characteristic of the bandpass filter during an adjustment where in actual operation second peak is adjusted and shifted to 100 Hz. This improvement is shown by comparing the ripple of Figure 16 and Figure 17 where Figure 16 shows the ripple with active filter and Figure 17 does without active filter. A 50 Hz ripple is reduced by 34 dB and a 100 Hz ripple is reduced by 45 dB. Beside the 50 Hz and 100 Hz, the suppression of ripples of other harmonics are all improved up to the fundamental logical harmonic.

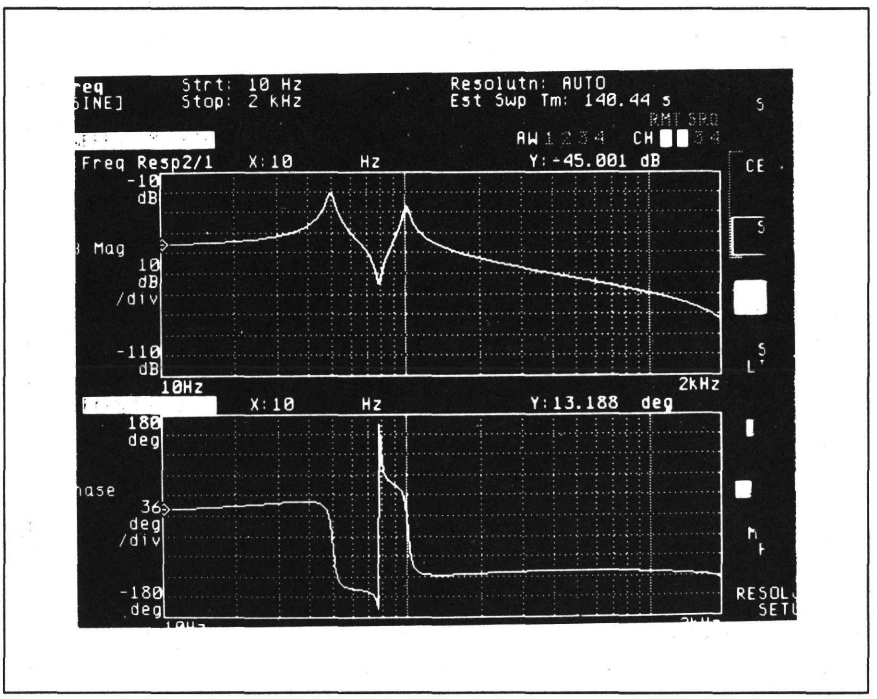

FIGURE 15. Frequency characteristic of the Banpass filter in the Active Filter.

HIMAC has two dipole power supplies (2x5 MVA) and four quadrupole power supplies (4x500 kVA). Two rings operate out-of phase. The magnitude of the illogical ripples also fluctuates by a few dB. In Figure 18, the voltage

ripple of a one-turn coil of a magnet yoke of Defocussing Quadrupole (upper trace) and Focussing Quadrupole (lower trace) is displayed to show how much the fundamental logical harmonic of 1200 Hz is reduced compared to that of the input of the ladder circuit load. A reduction of 15 dB is seen which brings down the relative ripple of about 0.05 ppm. The difference of a magnitude of 100 Hz ripple between the two is due to an absence of bandpass filter in the power supply of Defocussing Quadrupole.

DC Operation

For comparison, the spectrum of the voltage ripple of the normal mode in DC operation is shown in Figure 19, Figure 20 and Table 1. The amplitude of the ripple is smaller by several dB than that of the pattern operation. In case of the pattern operation, the ripple is measured at the flat top of the trapezoidal pattern. At the beginning of the flat top, the transient oscillation due to a rapid change of the pattern voltage can not be avoided. In Table 2 and Table 3 the 50 Hz ripple and 100 Hz current ripple are shown for various excitation levels respectively. As these current ripples are caused by unbalance and imperfections of the ac transformer and the triggering timing, the magnitude of the ripple can not be predictable and differs between the Upper ring and the Lower ring. They also depend on the excitation level.

Comparison of Illogical ripples

Illogical ripple is produced by the imbalance of the voltage and trigger timing among the 24 thyristor blocks as well as the imbalance of primary ac line. The relative magnitude of the ripple content of the six power supplies are shown in Figure 21 for several excitation levels. Their values are dependent on the operating condition. In this case, all six power supplies were turned on simultaneously. The data was taken during the tuning of the power supplies and associated numbers do not necessarily mean their optimized value but still give us a measure of performance. From the Figure 21, it turns out that the magnitude of the 50 Hz ripple of the Bending Magnet Power Supply of the lower ring is much greater than that of the upper Ring. And the excitation dependance of the lower ring is stronger than that of the upper ring. Later it turned out that the larger ripple of the Bending Magnet Power Supply is related to the poorer beam spill of the lower ring until we realized that the tolerance of the Bending Magnet Power Supply must be as good as that of the Focussing Quadrupole Magnet Power Supply.

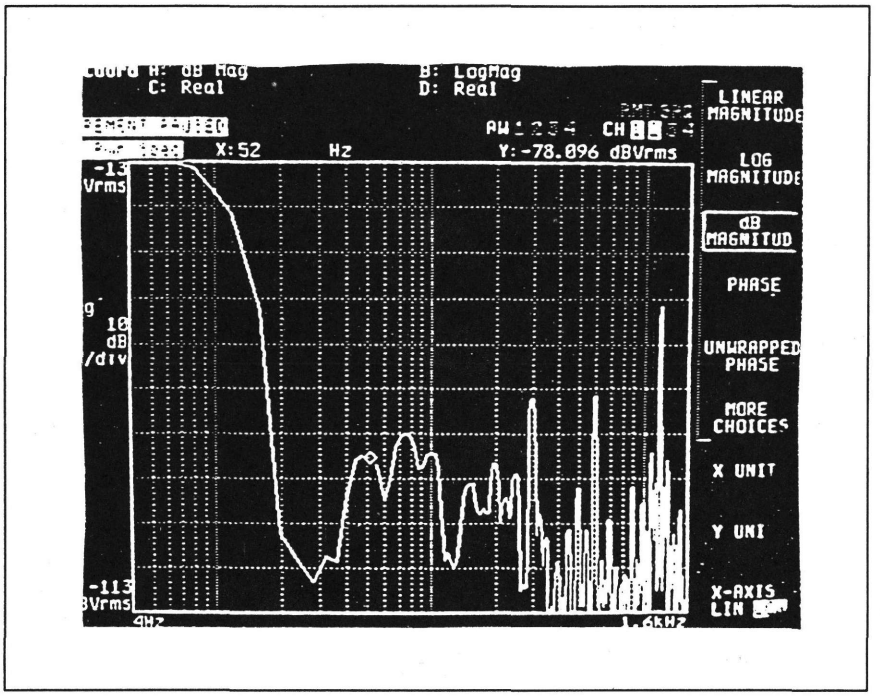

FIGURE 16. Normal mode voltage ripple with active filter (290 MeV/u) of the Focusing Quadrupole. The frequency covers from 4Hz to 1.6 kHz.

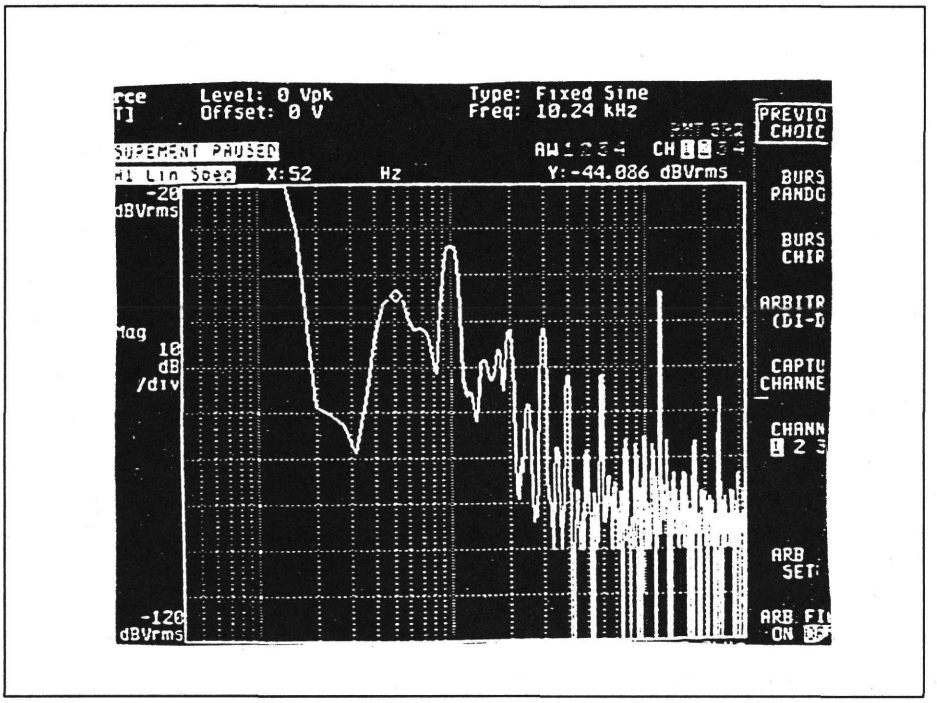

FIGURE 17. Normal mode voltage ripple without active filter (290 MeV/u) of the Focusing Quadrupole. The frequency covers from 4Hz to 3.2 kHz.

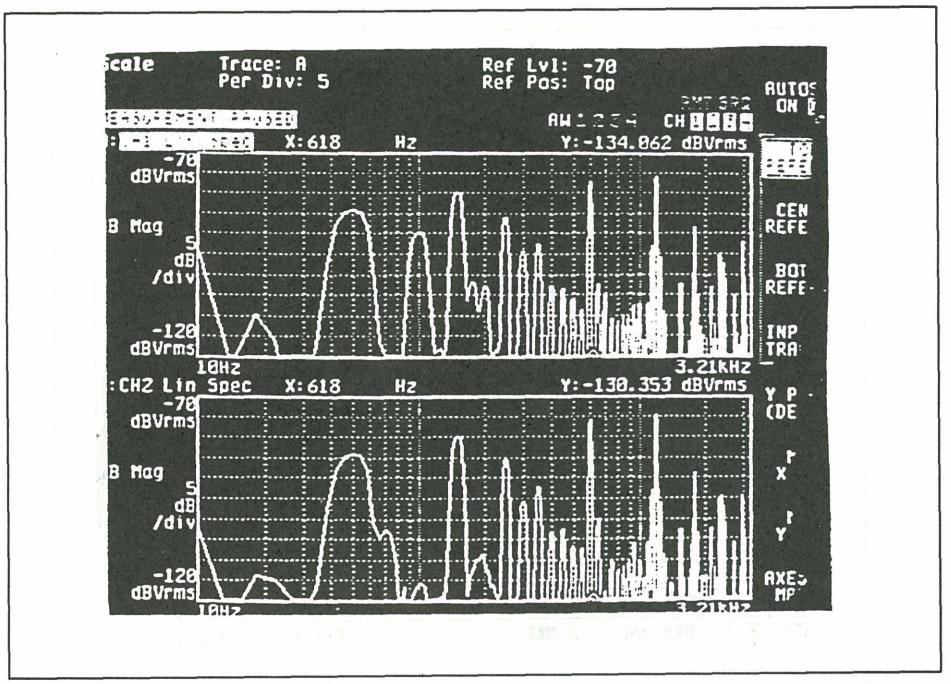

FIGURE 18. Output voltage of one-turn coil QD(upper trace) , QF (lower trace). The frequency covers from 10 Hz to 3.2 kHz.

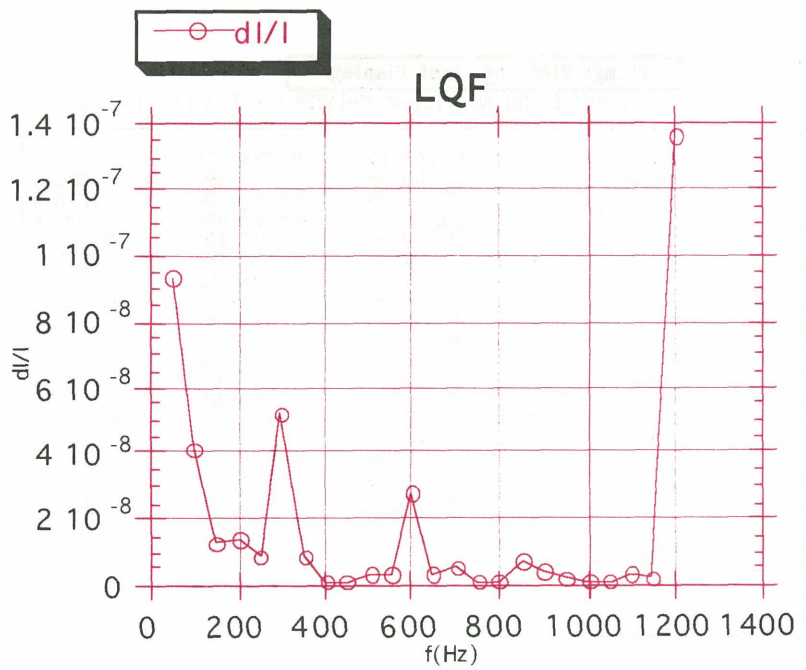

FIGURE 19. Relative current ripple of the Focussing Quadrupole.

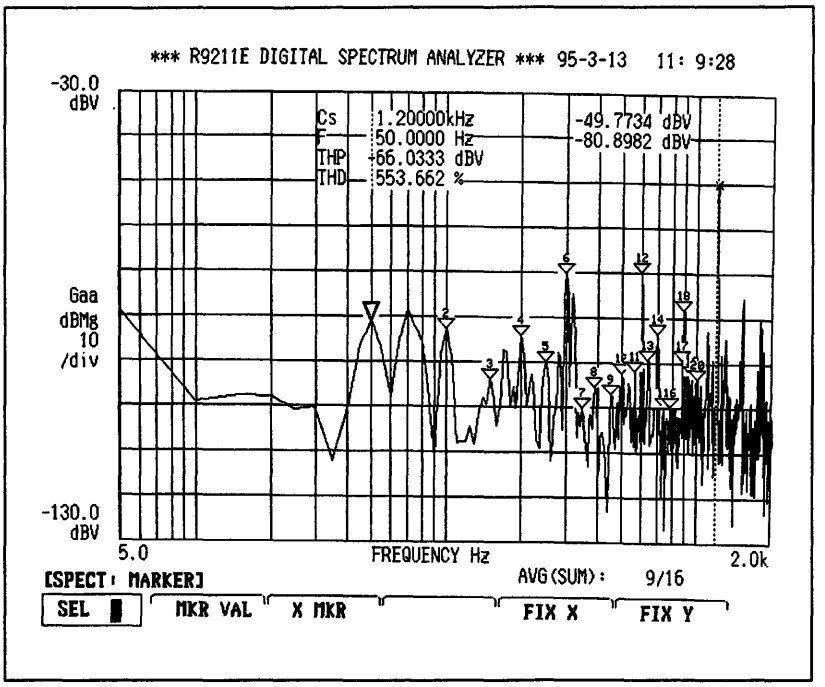

FIGURE 20. Spectrum of the Focussing Quadrupole of DC operation. I= 800A.

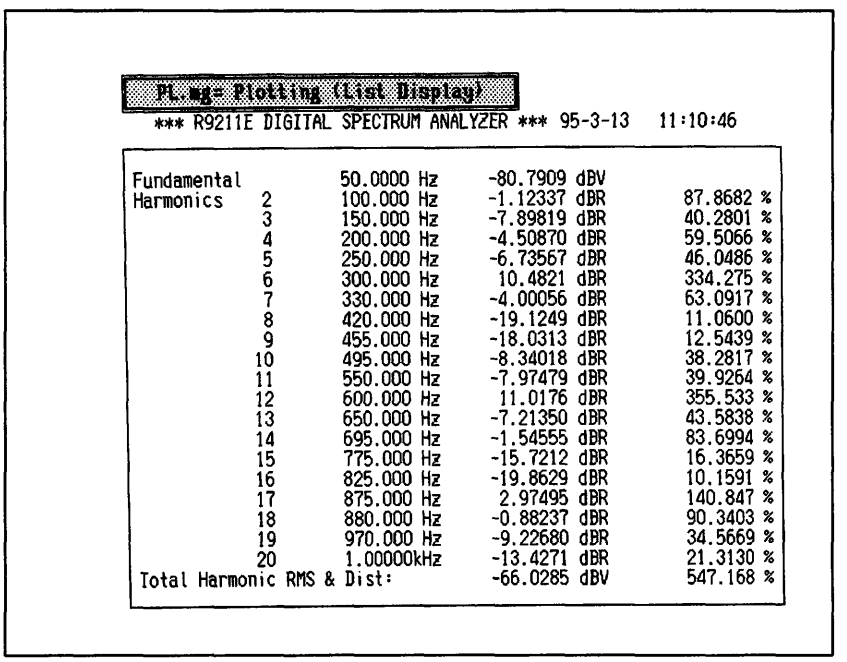

Fundamental		50.0000 Hz	-80.7909 dBV	
Harmonics	2	100.000 Hz	-1.12337 dBR	87.8682 %
	3	150.000 Hz	-7.89819 dBR	40.2801 %
	4	200.000 Hz	-4.50870 dBR	59.5066 %
	5	250.000 Hz	-6.73567 dBR	46.0486 %
	6	300.000 Hz	10.4821 dBR	334.275 %
	7	330.000 Hz	-4.00056 dBR	63.0917 %
	8	420.000 Hz	-19.1249 dBR	11.0600 %
	9	455.000 Hz	-18.0313 dBR	12.5439 %
	10	495.000 Hz	-8.34018 dBR	38.2817 %
	11	550.000 Hz	-7.97479 dBR	39.9264 %
	12	600.000 Hz	11.0176 dBR	355.533 %
	13	650.000 Hz	-7.21350 dBR	43.5838 %
	14	695.000 Hz	-1.54555 dBR	83.6994 %
	15	775.000 Hz	-15.7212 dBR	16.3659 %
	16	825.000 Hz	-19.8629 dBR	10.1591 %
	17	875.000 Hz	2.97495 dBR	140.847 %
	18	880.000 Hz	-0.88237 dBR	90.3403 %
	19	970.000 Hz	-9.22680 dBR	34.5669 %
	20	1.00000kHz	-13.4271 dBR	21.3130 %
Total Harmonic RMS & Dist:			-66.0285 dBV	547.168 %

Table1. Magnitude of the Harmonics of Focussing Quadrupole of DC operation. DBR means relative dB from dB of 50Hz.

50Hz ripple	DC60%	290MeV/u	600 MeV/u	800 MeV/u
UBM (ppm)	1.5	0.6	1.4	1.5
LBM(ppm)	5.0	4.3	6.7	2.9

Table 2 50 Hz ripple in Bending Magnet Power Supply

100 Hz ripple	DC60%	290MeV/u	600 MeV/u	800 MeV/u
UBM (ppm)	6.7	3.2	4.5	6.5
LBM(ppm)	8.7	2.8	3.9	4.3

Table 3 100 Hz ripple in Bending Magnet Power Supply

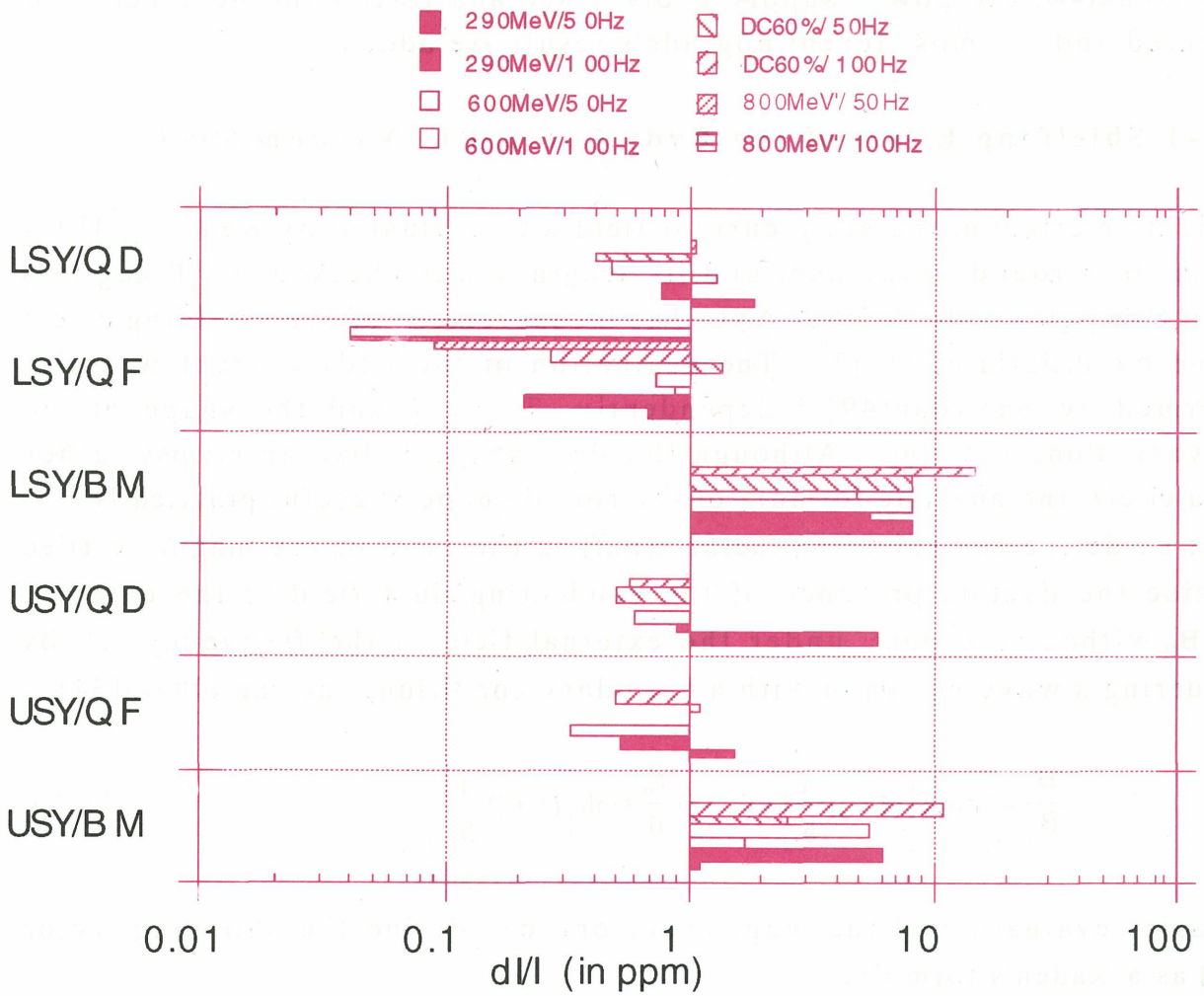

FIGURE 21. Comparison of the Current Ripple among six Power Supplies. During the process of further upgrade of the lower ring Bending magnet, the ripple current is now as low as 0.2 ppm.

VIII. Discussion

Mechanism and implementations to reduce the logical,illogical ripples and the spike in a synchrotron power supply system are studied in detail in preceding chapters. The final goal is to obtain a uniformly slow extracted beam by reducing the ripples in the magnetic field B_i. Discussion so far was restricted to the magnetic field in an absence of a vacuum duct. In reality, inside the conducting pipe under the external field B_0, the magnetic field is screened to some degrees, which depends upon the frequency and other factors such as a size and a thickness of a vacuum duct. In this chapter, this effect is first inspected, then the relation between the beam spill and the performance of the power supply is discussed,and finally the perspective is presented and the most recent upgrade's result are added.

VIII-1 Shielding Effect of the Eddy Current in Vacuum Duct

Shielding effect of the eddy current field was evaluated by Kaden [34] for the case of a round shape duct and its accuracy was checked by Praeg [35] by the Computer code PE2D at ANL. The measurement of the shielding effect is done by P.Burla et al. [36]. The evaluation of the eddy current was also performed by Snowdon[49] independently. The size and the shape of the duct vary along the ring. Although the duct shape is like an ellipse rather than a circle, the analytic formula of the round shape is useful practically.

Let us define the shielding factor $\varepsilon(r_o,f)$ as the ratio of the magnetic filed B_i inside the duct in presence of the conducting duct field to the external field B_o without the duct, under the external field of the frequency "f". By considering a wave equation with a boundary condition, one can obtain[34],

$$\frac{B_i}{B_o} = \left[\cosh\left[(1+j)\frac{d}{\delta} \right] + (1+j)\frac{r_o}{d} \sinh\left[(1+j)\frac{d}{\delta} \right] \right]^{-1}. \qquad (8\text{-}1)$$

For easier evaluation of the magnitude, one can define the shielding factor $\varepsilon(r_0,f)$ as a Kaden's formula,

$$\varepsilon(r_o,f)=\left|\frac{B_i}{B_o}\right|=\left[\left[\frac{r_o}{2\delta}\right]^2\left[\cosh\left[\frac{2d}{\delta}\right]-\cos\left[\frac{2d}{\delta}\right]\right]\right.$$
$$\left.+\frac{r_o}{2\delta}\sinh\left[\frac{2d}{\delta}\right]-\sin\left[\frac{2d}{\delta}\right]+\frac{1}{2}\left[\cosh\left[\frac{2d}{\delta}\right]+\cos\left[\frac{2d}{\delta}\right]\right]\right]^{-\frac{1}{2}} \qquad (8\text{-}2)$$

where r_o is a radius(cm) of the duct, d(cm) thickness of the duct,and $\delta(f)$ is a skin depth expressed by,

$$\delta(f)=\sqrt{\frac{\rho}{\pi\mu f}} \qquad (8\text{-}3)$$

where ρ the resistivity and μ is a permeability. For the frequency less than the cut-off frequency f_c, the above equation is simplified to,

$$\varepsilon_{low}(r_o,f)=\left[1+\left[\frac{r_o d}{\delta(f)^2}\right]^2\right]^{-\frac{1}{2}} \qquad (8\text{-}4)$$

with the cutoff frequency f_c of

$$f_c=\frac{4\rho}{\pi\mu d^2}. \qquad (8\text{-}5)$$

For the case of d=0.3 mm(Dipole duct), f_c=16.8 kHz and δ=2 mm, and for d=3 mm(Quadrupole duct), f_c= 1.68 MHz and δ=0.15 mm where ρ= 1.2610^{-8} Ωm are assumed. Frequency characteristic of the shielding factor $\varepsilon(r_0,f)$ is plotted in Figure 24 and Figure 25. Appreciable amount of shielding effect is seen for 3 mm duct(Quadrupole) and not much for the 0.3 mm duct(Bending magnet).

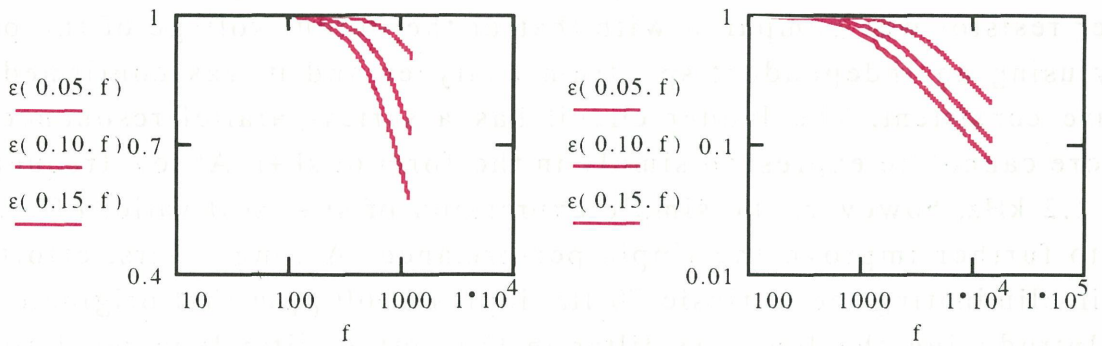

FIGURE 22. Frequency characteristics of the Bending Magnet's shielding factor for the radius of r_o= 5, 10,15 cm from the top trace to the bottom (d=0.3 mm).

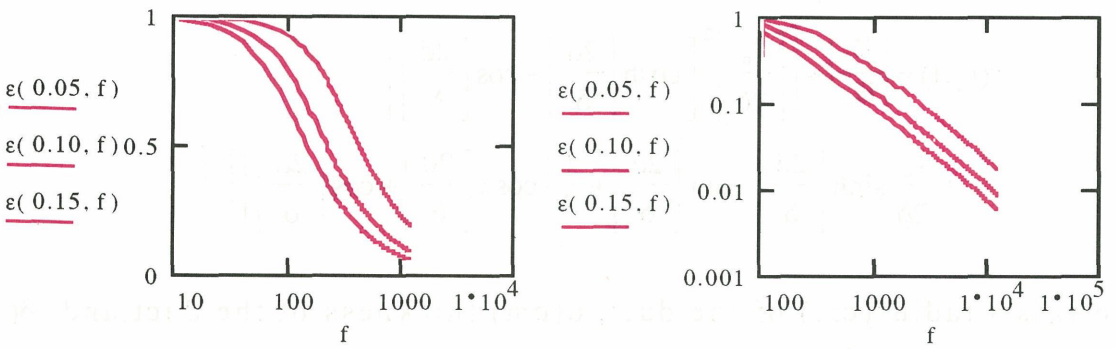

FIGURE 23. Frequency characteristics of the Quadrupole's shielding factor ε(r,f). The radius r_o= 5, 10,15 cm are from the top to the bottom (d=3 mm).

VIII-2 Beam Spill and the Ripple of the Magnet Power Supply

Efforts were made to suppress the magnitude of the ripple content of the Quadrupole Magnet Power Supply. Considering that the inductance of the Bending magnet is six times larger than that of the Quadrupole, and the magnitude of the illogical harmonic current is inversely proportional to the inductance at low frequency and furthermore as the ripple tolerance of the power supply of the Bending magnet is considered to be less stringent than that of the Quadrupole, the active filter was incorporated to the Power Supply of the Quadrupole Magnet alone at the beginning. Although the magnitude of the ripple content of the Quadrupole Magnet was at level of a few ppm, at the commissioning stage, the beam spill was not so uniform contrary to the expectation. This unsatisfactory spill was attributed to 50 Hz and 100Hz ripples of the Focussing Quadrupole magnet, rather than the accuracy of the measurement. Spectrum of the voltage of the accurate breeder resistor was compared with that of the output voltage of the power supply using an independent spectrum analyzer and it was confirmed that they are consistent. The ladder circuit has a series-parallel resonance and therefore cannot be expressed simply in the form of sL+r. At low frequencies below 1.2 kHz, however, the simple expression of sL+r still valid. Effort was made to further improve the ripple performance. Among others, efforts wa made in eliminating the intrinsic 50 Hz ripples of 60 ppm that originate from DCCT. Introducing the low pass filter in the active filter loop resulted in a reduction by 20 dB. The addition of the bandpass filter of the 50 Hz and 100Hz in parallel to the high pass filter in the lower synchrotron's Focussing Quadrupole, was also effective in further reducing the ripples by 20 dB. The

relative ripple level normalized by the rated current was 0.3 ppm.

Contrary to the achievement of a significantly lower level of ripple in the Quadrupole of the Lower Ring, the spill of the Lower Ring was not improved as expected. Figure 24 represents the beam spill of the Lower Ring. Figure 26 represents that of the Upper Ring after the extensive improvements. There was a fluctuation of about 5 dB in the magnitude of the ripple due to the inter-coupling of the power supplies or an adjustment. The ripple of the Quadrupole of Lower Ring is better than that of the Upper Ring. The spill of the Upper Ring, however, was better than that of the Lower Ring. This contradictory observation was studied by the applying the "Ripple Basher". Ripple Basher, whose signal is the harmonic signal of the multiples of 50 Hz is fed to the power supply. The correlation between the spill and the Ripple Basher signal is studied. The effort of improvement was concentrated on the Upper Ring because the priority was given to reproducible spill of the Lower Ring due to the requirement of the medical use. In comparing the spill before and after the improvement of Lower Ring, a major difference in the amplitude of the frequency of 50 and 100 Hz is seen. Even after the improvement in these ripples, a uniform spill was not obtained. This contradictory observation can be explained as follows; the 100Hz component is composed of two components of the 50 Hz spill from different source. By eliminating one of the ripple sources, and leaving the another source untouched,the 50 Hz ripple was still observed.

To identify the ripple source other than that of the Focussing Quadrupole, small amount of signal from the Ripple Basher was added into the Input of the Focussing Quadrupole's minor AVR. Its effect was detected as the ripple in the beam spill as shown in Figure 27. Externally added 50 Hz signal by the Ripple Basher(bottom trace) corresponds to the smaller peaks appearing between the larger peaks of the unknown source. By shifting the phase, the correspondence between the signal of the Ripple Basher and the change in the ripple in the spill was confirmed. In a similar way, the signal from the Ripple Basher whose order of the magnitude corresponds to that of the ripples of the Bending Magnet Power Supply is added to the Input of the minor AVR of the Bending Magnet Power Supply. The effect of the ripple in the Bending Magnet was clearly observed. The ripple of a few ppm level in Focussing Quadruple Power Supply and that of 10 ppm in Bending Magnet Power Supply result in a considerable amount of ripple distortion.

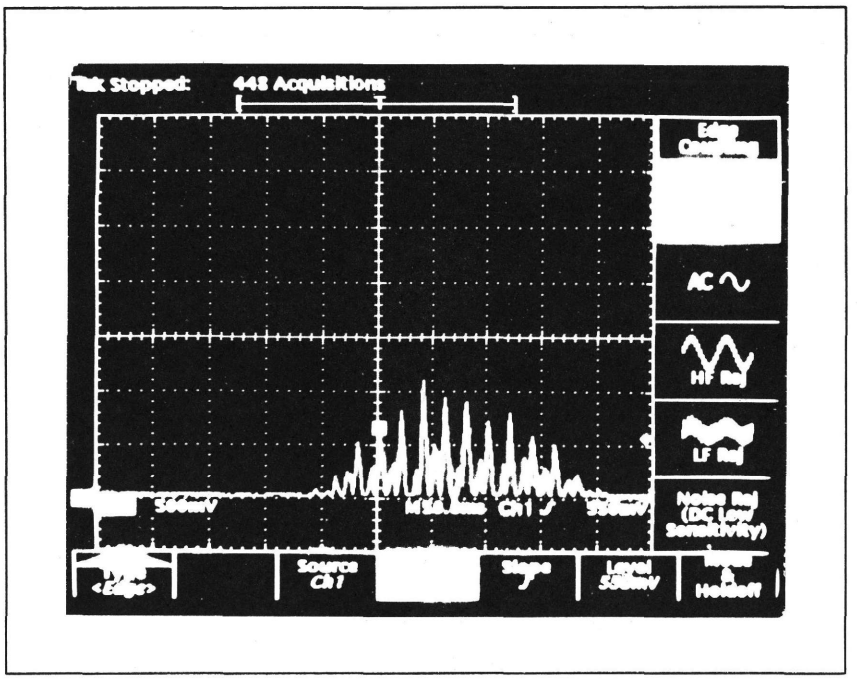

FIGURE 24. Typical beam spill of the Lower Ring at 400 MeV/u during the period of one year in the period of commissioning. (50 ms/division)

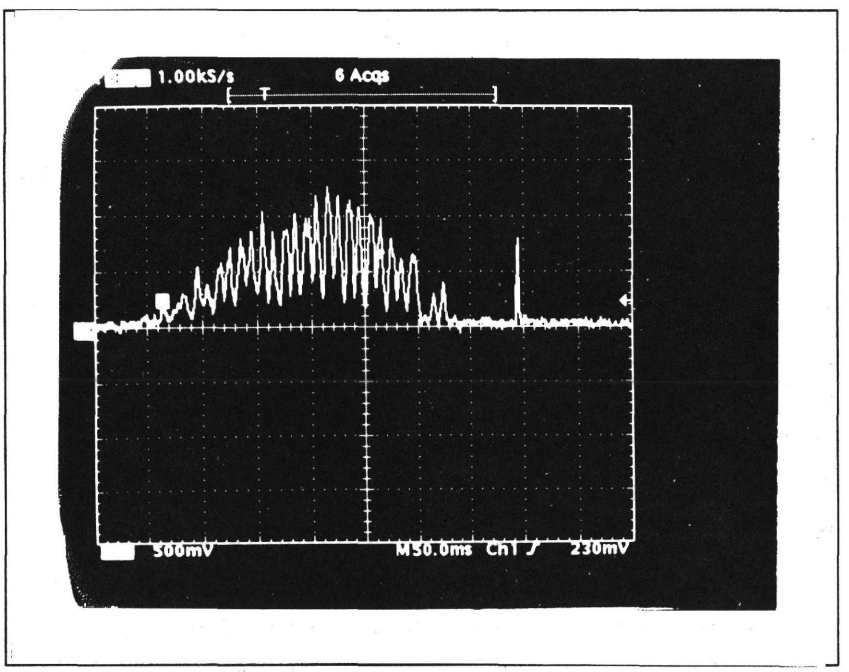

FIGURE 25. Typical beam spill of the Upper Ring at 400 MeV/u.(50ms /division).

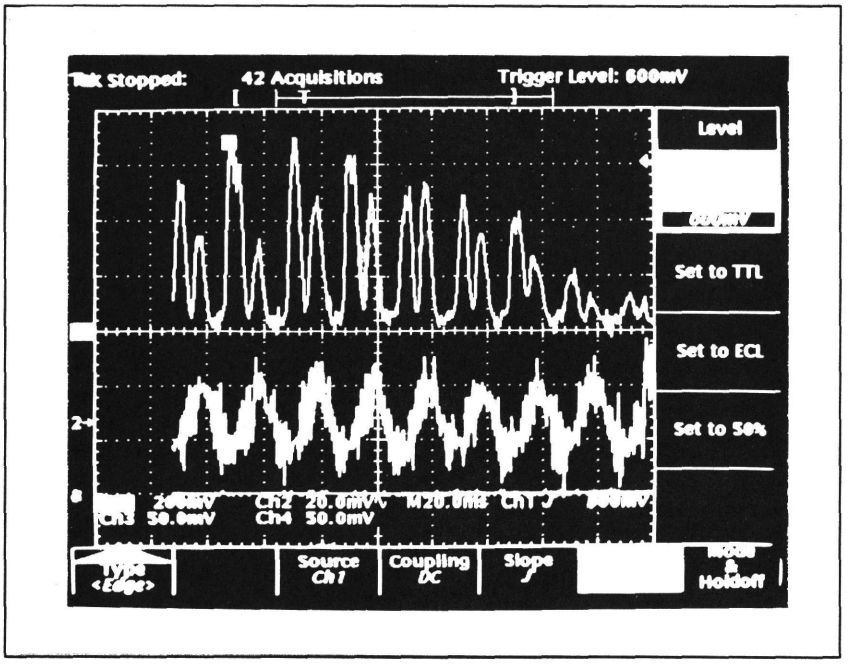

FIGURE 26. Beam spill and the voltage ripple of the Focussing Quadrupole of the Lower Ring at 400 MeV/u after the improvement. The upper trace shows the beam spill and the lower trace shows the voltage ripple in the Quadrupole Magnet power supply.

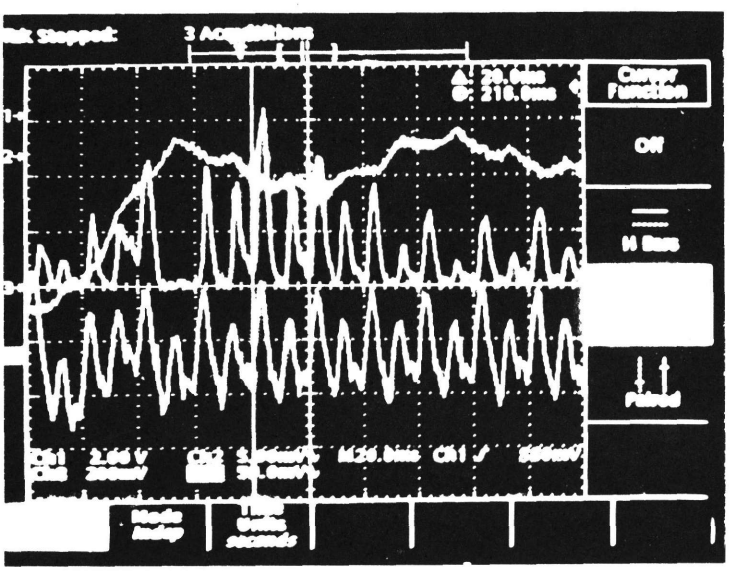

FIGURE 27. Evidence of the Synchronization of the Dipole Ripple and the spill ripple. From the upper, the middle and the lowest traces are the voltage ripple of the Quadrupole Power Supply, beam spill and the voltage ripple of the Bending Magnet Power Supply of the Lower Ring at 400 MeV/u.

Finally a full evidence of the synchronization between the Bending magnet Ripple and the spill ripple was observed as shown in Figure 27. Figure 28 shows the corresponding ripple magnitude. Figure 27 shows perfect synchronization between the beam spill and the ripple voltage of the Focussing Quadrupole. In this operation, the Ripple Basher was switched off. The upper trace is the ripple, 0.6 ppm, in the Focussing Quadrupole Power supply, the middle trace is the beam spill, the lowest trace is the ripple, 10 ppm, in Bending Magnet Power supply in Figure 27. On the other hand, the effect of the ripple of the Quadrupole is not seen in the beam spill at all. This means the magnitude of the ripple is small enough to be detected and the requirement for it is completely satisfied. However, it was found that the effect of the ripple in the Bending Magnet was under-evaluated. This was not found until the ripple performance of the Quadrupole Power Supply went to the sub-ppm level. When the magnitude of two ripples of different sources are similar, the effect mixes, and a definitive conclusion may not be drawn. The mechanism of the effect of the ripple of the Bending Magnet Power Supply to the beam spill is considered to be through Sextupole Magnet located in the ring to compensate the natural chromaticity of the synchrotron. Variations in the dipole field cause variations in the orbit of the beam, and this displacement in the orbit in the Sextupole Magnet causes the variation of the quadrupole component that is a linear function of the displacement. Rough estimation of the tolerance of the Bending Magnet Power Supply shows that it is comparable to that of the Focussing Quadrupole when the Sextupole is operated to fully compensate the natural chromaticity. In this naive picture of the tune variation, the field strength in the Sextupole is decreased while the strength of the Quadrupole is adjusted so that the spill intensity does not decrease. Considerable amounts of improvement in the beam spill is confirmed as shown in Figure 30 and Figure 29 where the spill of the Upper Ring corresponds to the energy of 350 MeV/u and that of the Lower Ring to the energy of 400 MeV respectively.

VIII-3 Progress and Future Improvement

Discussion above indicates that by improving the normal mode 50 Hz and 100 Hz, higher harmonic ripple and spike are almost completely removed as expected by a modal analysis of the ladder circuit of the three input and output. The first improvement of the beam spill was done by improving the

Qaudrupole power supply ripple. Due to the under-evaluation of the ripple in the Bending Magnet Power Supply during the design stage, the beam spill was rather poor. The next improvement was done by improving the Bending magnet power supply. The present beam spills shown in Figure 29 and Figure 30 show better improvement. They are stable and reproducible. Quality of the spill is not deteriorated at a lower energy level of 290 MeV. It is better at higher energies because of the smaller relative ripple level. It should be emphasized that this quality in the spill is realized solely by the Main Power Supply without having to resort to any other auxiliary means such as the spill feedback system with auxiliary devices that are necessary means in other synchrotrons. The current magnitude of the ripple of the Quadrupole Power supply promises even better quality of the beam spill when the ripple of the Bending Magnet Power Supply is improved. The improvement of the Bending Magnet Power Supply will be done by adding an active filter like the one applied to the Quadrupole Magnet Power Supply. The magnitude of the load's impedance in the Bending Magnet is larger by a factor of six, therefore it is probable that the relative magnitude of the sub-harmonics current ripple is expected to be less than that of the Quadrupole if the performance of the active filter is made to be the same.

Improvement in the Power Supply is possible by another mean; replacing the DCCT with better performance[43,44]. The present DCCT contains the intrinsic 50 Hz ripple of the order of 60 ppm and the intrinsic ripple of the new DCCT expected to be two orders of magnitude less for the ripple. It was found that the lower illogical ripples such as 50 Hz were mainly due to this intrinsic ripple. New DCCT has been tested and is promising. Figure 31 and Figure 32 show the voltage spectrum of the output of the power supply of the Bending magnet without the active filter and with the active filter. Considerable amount of the ripple reduction is seen. Using eq.(7-1), we get, 50 Hz-76 dBV(0.1 ppm),100Hz -62 dBV(0.2 ppm), 1200Hz-55dBV(0.1 ppm). With these improvement, the quality of the beam spill is expected to be more uniform and stable. During the period of preparing this article the upgrade of the power supply is underway, where bandpass filter upto 1200 Hz is provided. With these upgrade,the most recent uniform beam spill of the lower ring is shown in Figure 33. This beam spill is mainly due to the upgrade of the Active filter with better bandpass filter and new DCCT.

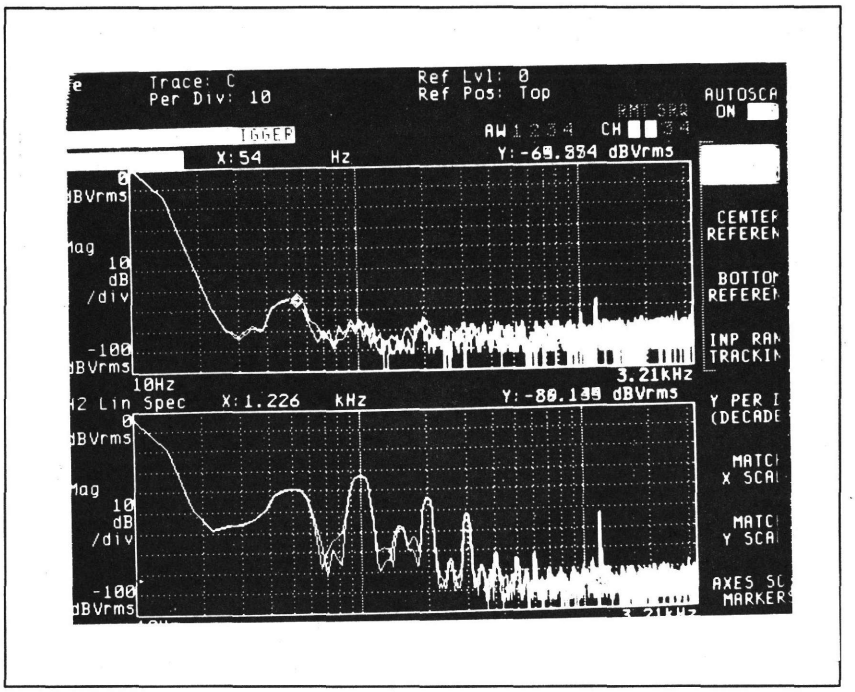

FIGURE 28. Spectrum of the voltage ripple of the Quadrupole Power Supply and that of the Bending Magnet Power Supply.

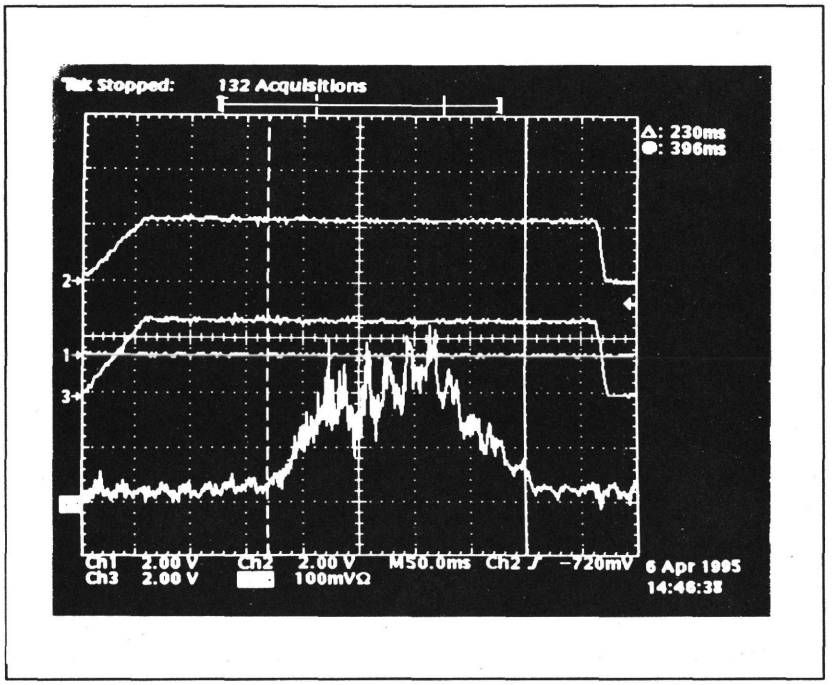

FIGURE 29. Beam spill of the Upper Ring at 400 MeV/u is shown at the lowest trace with sextuple current traces above. The fluctuation of the spill is attributed to the ripple of the Bending Magnet Power Supply.

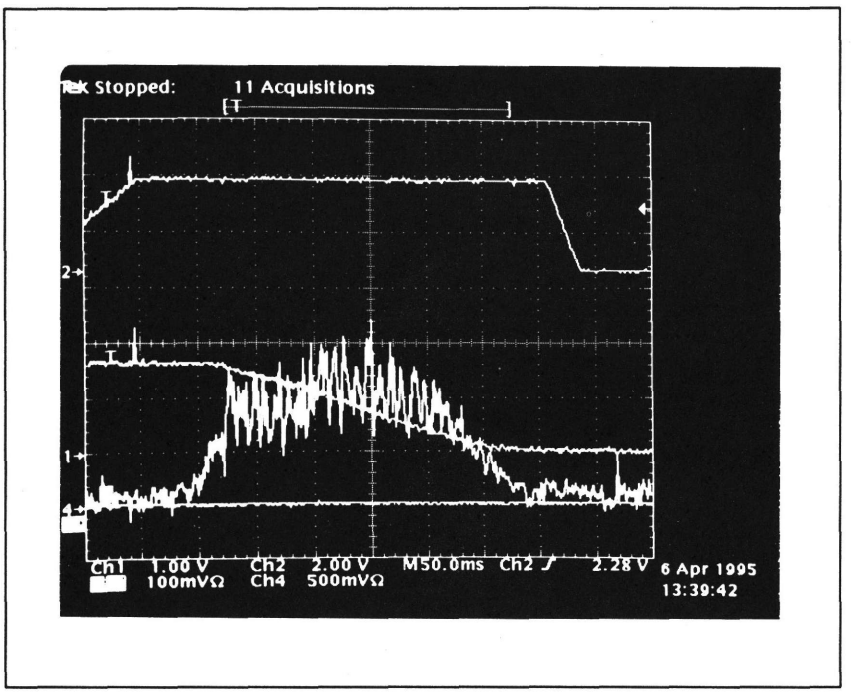

FIGURE 30. Beam spill of the Lower Ring at 400MeV/u at the lowest trace with traces of sextuple current. In both ring, no spill feedback or auxiliary devices are not used. Horizontal axis is in 50 ms/division.

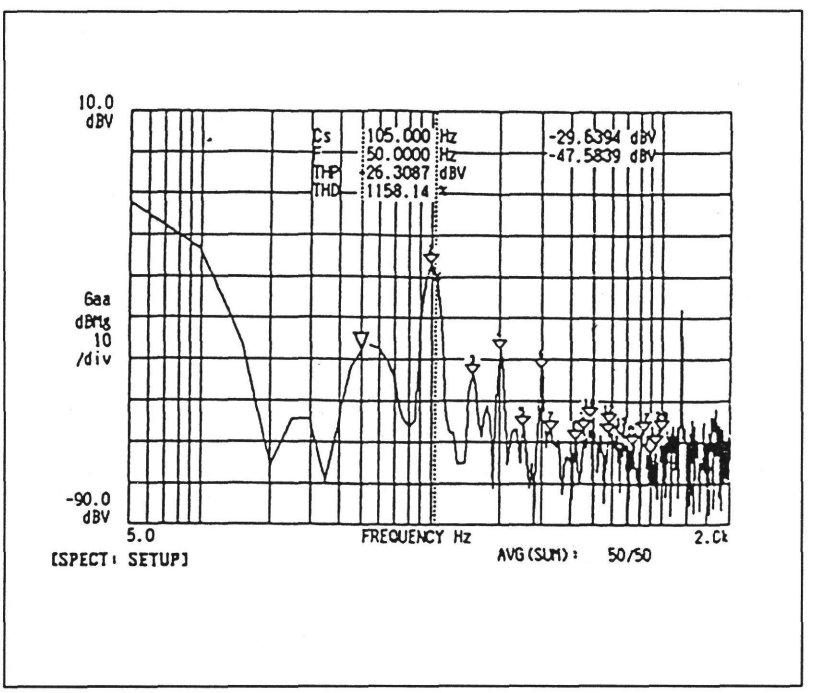

FIGURE 31. Typical voltage ripple of the output of Bending Power supply without Active Filter.

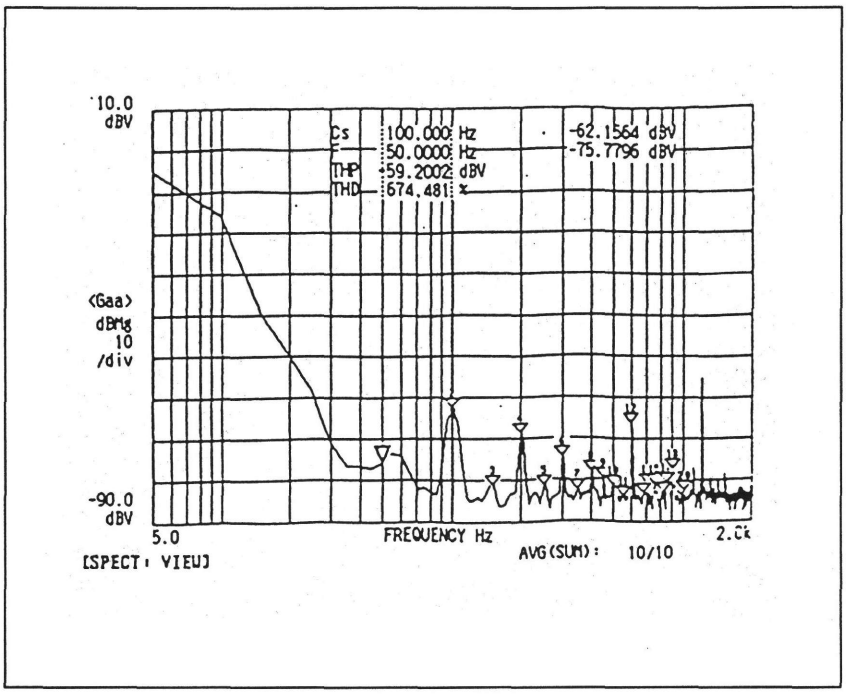

FIGURE 32. Typical voltage ripple of the output of Bending Power supply with Active Filter installed. 100 Hz is 0.2 ppm and the largest.

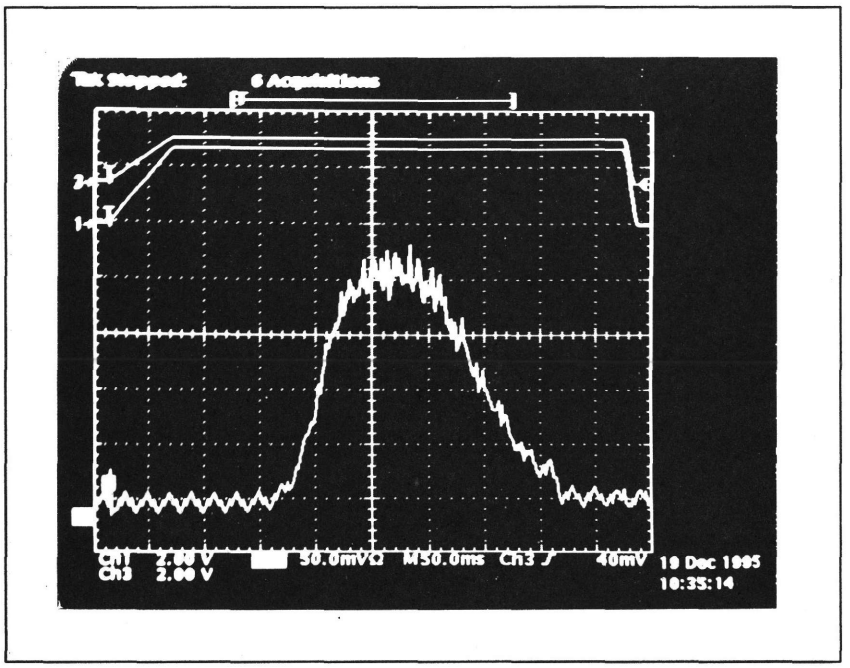

FIGURE 33. Recent Beam spill after the upgrade of the Quadrupole and Bending magnet power supply in the lower synchrotron ring. The lowest trace shows the beam spill. The upper and the second traces show the wave form of extracting sextupoles,SXFr and SXDr.

IX. Summary

As a summary, the characteristic features of this study are graphically shown in following two figures. Figure 34 is a simplified circuit diagram of most of other synchrotron power supplies and their load. In the figures, we have considered the stray capacitance from the coil to the magnet yoke. The midpoint of the load magnet is either floated($Z_E = \infty$) or terminated by the resistor($Z_E=R_E$) or directly grounded($Z_E=0$). The simplified circuit diagram of the HIMAC synchrotron main power supply is shown in Figure 35. The existing power supplies are floating from the earth. This is shown is Figure 34 by a capacitance to the earth from the mid-point of the voltage source. In the HIMAC the midpoint is grounded. The grounding is necessary to form a common mode filter. Using this ground reference, we chose a single point earth.The earth of the power supply circuit and the load magnet is connected to this single earth.The bus bar earth line is running inside the power supply cubicle. The earth line is made to run along the excitation cables of the magnet string. These two bus bar earth line and the other earth line running in the synchrotron ring is connected together at the single earth point. Furthermore, the earth of the low level control circuit is connected to this earth. This grounded voltage source causes the increased common mode noise current in the earth line. The increased noise in the earth line simultaneously means a localization of the noise inside the earth line. This, in turn, made it possible to realize a low noise synchrotron power supply when it is looked from outside of the power supply system. The increased common mode noise current in the ground line is blocked and cannot enter into the magnet coil because of the common mode filter employed in the HIMAC. In the existing floating power supplies without a common mode filter and the earth line, the path of the common mode current is obscure and the noise current can not be confined in the power supply.

Magnet load of synchrotrons is regarded as a string of ladder circuit or transmission line type LCR circuit. The ladder circuit has a property of plural numbers of series and parallel resonance. The power supply has a resonance property. There is also a resonance between the ladder circuit and the power supply. In the past, only the normal mode of the magnet string is considered. The common mode ripple current, however, plays a significant role in a frequency range above a few kHz unless the attention is paid.

In the HIMAC, the load of the magnet string is carefully configured so that it is highly symmetric with respect to the ground line. The coils of the unit magnet is separated into upper coil and the lower coil. This separation results in higher symmetry and also magnetic coupling between the upper and the lower coil. This coupling further reduces the common mode impedance of the magnet and also suppresses the effect of the common mode to a magnetic field in the gap due to canceling effect by the currents of opposite direction. In a magnet string of other synchrotron, a degree of symmetry is obscure. In this case, the two mode of the normal and the common mixes. In the HIMAC, the mixing effect is expected to be much smaller than the existing magnet string. If the common mode is transformed into the normal mode, one can not suppress this component by the normal mode filter as the common mode filter is not provided. The mode mixing requires the necessity of the common mode low pass filter. In addition, the mode separation of the normal and the common may not be as useful as in the case of the HIMAC without the mode filters.

Role of the bridge resistor to the ripple and spike generation is clarified by the mode analysis. The symmetric configuration makes it possible to decouple the variables of U, V, I and J into two decoupled mode of the normal mode of (U+V) and (I+J) and the common mode of (U-V) and (I-J). The author established a formulation for the ripple current and spike current in presence of the bridge resistor where the details are described in the accompanying paper. With the aid of the analysis, the magnitude of the ripple and the spike are studied and evaluated and the magnitude of the bridge resistor is determined.

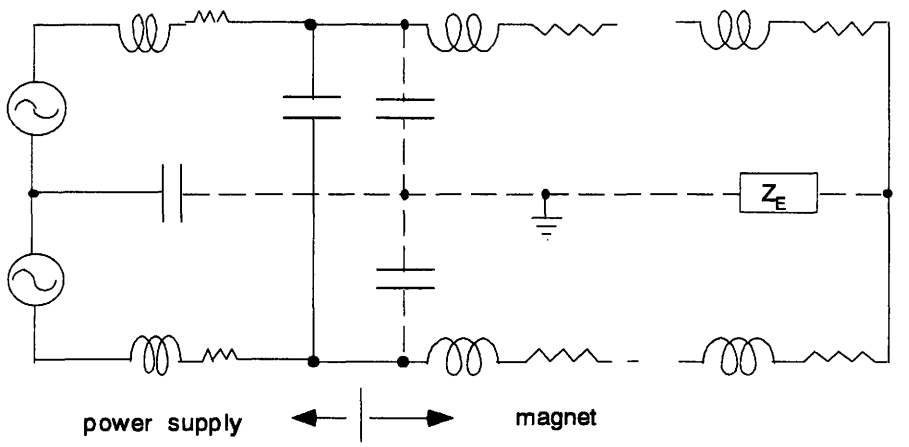

FIGURE 34. Most of other power supplies and their load. Voltage source is floated and the load is connected to the ground through the impedance Z_E which may be a resistor, shorted or opened.

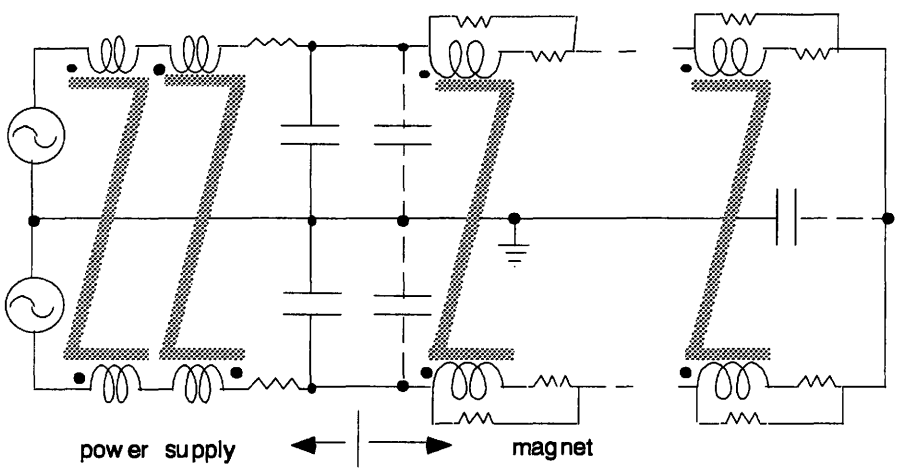

FIGURE 35. HIMAC power supply and its load. The voltage source is grounded. Normal and common mode filter is equipped. The upper and lower coil of the magnet is separated and magnetically coupled. Bridge resistor is installed.

Cross-over point of the normal mode and common mode admittance about a few kHz in case of without bridge resistor. Below this frequency, the common mode is less important. Due to the normal and common mode filter, for the ripple whose frequencies above 200 Hz is damped in both mode. With bridge resistor, the common mode admittance is less than the normal mode over a frequency range of interest, up to 50 kHz. With the static filter

of the normal and the common, most of the frequency component of a relative ripple current is below a level of a few times 10^{-7} in both mode except 50 Hz and 100 Hz of the normal mode. The 50 Hz relative ripple current of the Bending magnet power supplies was between 0.6 to 1.5 ppm for upper ring and 3 to 4 ppm for the lower ring. The 100 Hz ripple current was 3 to 7 ppm for the upper ring and 3 to 4 ppm for the lower ring. These performance was realized by the static filter alone.

The normal mode 50 Hz appeared in a pattern current where the intrinsic ripple of the DCCT output into digital repetitive feedback system. This is suppressed by shifting the cut-off frequency of the digital filter from 50 Hz to 25 Hz. The output of the same signal was output to the active filter system and caused a similar problem. This was again cured by the analog low pass filter of the same cut-off frequency. The bandpass filter of 50 Hz was also introduced in the Active Filter system and shown to be effective, roughly 10 dB.

Active filter was concentrated to suppress 100 Hz ripple. The normal mode 100 Hz was suppressed by the feed forward type Active Filter. Initially it is installed to the Quadrupole Magnet power supply and later installed in one of the Bending magnet power supply. The effect of the bandpass filter of 100 Hz is about 20 dB. In total, the reduction of the 50 Hz ripple voltage is 45 dBV for the Quadrupole power supply and 34 dBV for 100 Hz. The reduction of the ripple voltage for the Bending magnet power supply is 18 dB for 50 Hz and 32 dBV for 100 Hz.

Bridge resistor, the coil separation, the addition of the common mode filter and the single point grounding of the power supply and the load are all static method, nevertheless resulted in an excellent performance in ripple and spike current above 200 Hz in the HIMAC. The normal mode 50 Hz and 100Hz are the only ripple that can not be suppressed by the static method. 50 Hz ripple was confirmed to be removed by identifying its source and replacing it by other device of higher quality available on the market[43,44]. The active filter was concentrated to suppress 100 Hz ripple. And it was reduced to a level below ppm by the active filter.

X. Conclusion

Applying the general concept of "symmetry" and "mode decoupling " as the guiding principle in the design of the power supply, the bridge resistor,

separate connection of the coil and the common mode filter in addition to a normal mode filter can be a strong guiding principle in design of the synchrotron power supply. In particular importance of the symmetry is emphasized. From this viewpoint, the spacing of the gap between the coil and the yoke must be controlled to be uniform to realize symmetric capacitance. All the logical and most of the illogical ripples of the Quadrupole power supply can be reduced to a negligibly small level. 100 Hz ripple is also eliminated. 50 Hz problem was solved. Furthermore due to the common earth line of the power supply and the load, which is consequently introduced through the property of the "symmetry", the whole system can be made "noiseless" when seen from outside the power supply because the noise current is confined to flow only through the earth line of the power supply. The symmetry allows for the decoupling of individual systems such as the low level power supply of the control circuit. Owing to the study described, a highly reliable power supply and the magnet system could be constructed with considerable suppression of the logical ripple and the thyristor spike. The level of the final illogical ripple level could be as low as below ppm. With the realization of a low level of ripple and good beam spill, the design principle of this research can be said to be appropriate and the goal of this research is attained.

XI. Acknowledgement

The author would like to express their thanks to Director General Y.Hirao and Director K.Kawachi for their continuing support and encouragement. This paper would not be completed without the patient guidance and discussions with Prof.K. Sato of University of Osaka and Prof.S.Matsumonto of Dokkyo Medical University. Discussions were beneficial with Drs.K.Noda,E.Takada, M.Kanazawa,S.Yamada,A.Itano of the HIMAC. The author also likes to thank his collaborators who assisted during the construction of the HIMAC, such as Drs.Y.Irie, S.Watanabe, H.Sato, T.Sueno. This work could not be completed without the cooperation of the Physics and Engineering Division Group and T.Aoki of Accelerator Engineering Corporation. Finally, the discussion with H.Kubo of Hitach Ltd., who manufactured the system was inevitable. The author thanks Dr.H.Bicshel of NPL, University of Washington and S. D.Whitehead for revising the manuscript.

XII. References

[1]P.J.Bryant,"Performance requirements for accelerators", CERN Accelerator school, Power convertors for particle accelerators, CERN 90-07,1990, pp.1-15.
[2]H.W.Isch,J.G.Pet and P.Proudlock,"An overview of the LEP power converter system", CH2387-9/87/0000-1399 IEEE,PAC 87, pp.1399-1401.
[3]A.Dupaquier,P.Proudlock,"Switch-mode power converters",CERNAcc. school, Power convertors for particle accelerators,CERN90-07, 1990, pp.103-120.
[4]Y.Shoji, as for BNL, H.Sato and T.Sueno as for KEK, Private communication.
[5]P.Proudlock,"Achieving high performance", CERN Accelerator school, Power convertors for particle accelerators, CERN 90-07,1990, pp.55-79.
[6]R.E.Olsen,"A high performance digital triggering system for phase controlled rectifiers",IEEE,Vol.NS-30, No.4, August 1983.
[7]R.Olsen and H.Langenback,"High precision power supplies for the National Synchrotron Light Source",CH2387-9/87/00000-1408,1987,PAC,pp.1408-1409.
[8]G.Bagley and R.J.Edwards,"CBA main magnet power supply ripple reduction", 0018-9499/83/0800-2923,1983 IEEE, p.2923.
[9] H.Sato and M. Masuda, "The dynamic filters for KEK main ring quadrupole magnets", KEK-76-20.
[10]F.F.Cilyo et al., "Active filter for high current dc magnets", IEEE,Vol. NS-28, No.3, June 1981, pp.3014-3016.
[11]H.Baba et al. "Improved dynamic filters for the Main ring magnet power supply of the KEK 12 GeV PS", IEEE, Vol.NS28, No.3, June 1981,pp.3068-3070.
[12]R.J.Yarema,"Subharmonic ripple reduction in SCR type magnet power supplies", NS-26, 0.3,June, p.3986(1979).
[13]D.Wolff et al.,"Improving regulation in the Fermilab main ring magnet power supply",vol.NS-28, No.3, (1981),p.2929.
[14]J.P.Aknin et al.,"Status report in rejuvenating SATURNE and future aspects", IEEE, Vol. NS-26, N0.3, June 1979, p.3138.
[15]W.Praeg,"A high-current low-pass filter for magnet power supply",IEEE transactions on industrial electronics and control instrumentation, Vol.IECI-17. N0.1, February, 1970.
[16]S.Matsumoto of KEK, now at Dokkyo Medical University,private communication.
[17]J.McCarthy et al., PAC85, 1985, IEEE, p.3779.
[18]M.Kumada,"Design of the HIMAC Synchrotron Power Supply",PAC93,

Washington DC, pp.1291-1293.
[19]E.Regenstreif,"The CERN proton synchrotron(1 st part),CERN59-29, pp.153-158.
[20]S.Van der Meer,"Delay line effects in the 300 GeV magnet circuit", ISR-PO/S, MC/12,October 22,1969.
[21]R.E.Shafer,"Eddy currents, dispersion relations and transient effects in superconducting magnet", IEEE Transaction on magnets, Vol.MAG-17, No.1, January 1981, pp. 722-725.
[22]R.E.Schafer,"Transmission line property of long strings of superconducting magnets",IEEE Vol.MAG-17,NO.1, Jan. 1981, p.726.
[23]K.M.Smedley, R.E.Shafer,"Measurement of AC electrical characteristics of SSC superconducting dipole magnets", p.629.
[24]R.E.Schafer,K.M.Smedley,"Electrical characteristics of long strings of SSC superconducting dipoles", HEACC'92, HAMBURG, pp.298-300.
[25]O.Calvo,G.Tool,"Analysis of transmission line effects in the SSC magnet system",Fermilab,CH2387-9/87/0000-1425,1987 IEEE particle accelerator conference, Washington D.C., pp.1425-1427.
[26]H.J.Eckoldt,"Simulation of transmission line effects within an octant of the superconducting HERA ring during an energy ramp", DESY, HEACC'92 , HAMBURG, pp.329-331.
[27]R.Bacher et al.,"Transmission line characteristics of the S.C. HERA dipole and Quadrupole string", HEACC'92,HAMBURG, pp301-303.
[28]P.Burla et al.," Power Supply Ripple Study at the SPS",CERNSL/94-11(AP).
[29]M.Kumada et al., "System design of main magnet power supplies of the HIMAC heavy ion synchrotron,"The 8th Symp. on Accelerator and Technology, 1991, Saitama, Japan, p.199.
[30]M.Kumada et al.,"Analysis of the HIMAC synchrotron power supply", The 9th Symp. on Accelerator and Technology, 1993, KEK.
[31]M.Kumada et al."The HIMAC Very Low Ripple Synchrotron ", EPAC,1994.
[32]K.Sato, et al.," Performance of SVC for HIMAC synchrotron power supply", '94 Meeting of Electric society of Japan.
[33]K.Sato et al.,"Development of the PLL clock pulse generator for a control of synchrotron magnet", (in Japanese), proceedings of Japan Electric Society '93.
[34]P.H.Kaden,"Wirbelstrome und Schrumung",SpringerVerlag,1959,pp.71-75.
[35]W.F.Praeg,"Resistivity,Hysteresis and Magnetization of 9% Stainless Steel as a function of Temperature and Its Electromagnetic shielding Effects in

Cylindrial Structures", CH1441-5/79/0000-1817.
[36]P.Burla et al.,"Power Supply Ripple Study at the SPS",CERN SL/94-11(AP).
[37]M.Kumada,"Mode Mixing in Synchrotron magnet power supply",to be published.
[38]M.Kumada,"Mode Analysis of Synchrotron magnet strings", to be published in the proceedings of Particle accelerator conference, PAC95, Dalas.
[39]M.Kumada, "Analysis of the Ripple Current in HIMAC synchrotron Power Supply", submitted to Particle Accelerator.
[40]M.Kumada et al.,"Recent improvement of HIMAC synchrotron", to be published in the 10th Syp. On Accelerator and Technology,1995, Hitachi Naka.
[41]M.Kumada et al.,"Detection of the ripple current of the Synchroptron Power Supply below ppm", to be published.
[42]M.Kumada et al.,"The HIMAC Very Low Ripple Synchrotron Part II", EPAC,1996. submitted for the publication.
[43]Van der Bek et al.,European Patent,"Measuring circuit for continuous, accurate measurement of direct alternating current", Publication number, 0 314 234 A1.
[44]Van der Bek et al., European Patent," Circuit for the detection of an asymmetry in the magnetization current of a magnetic modulator", Publication number, 0261707 A1.
[45]Y.Konishi,"Microwave circuit", (in Japanese) sougou-denshi publish ing,1993, p.90.
[46]Y.Ohno,"Theory of modern transient phenomena",(in Japanese), Ohm publishing,1994, pp.107-110.
[47]S.Miyairu,"Fundamental power electronics", (in Japanese), Maruzen Inc., pp.89-90.
[48]W.Praeg and D.McGhee,"Power supplies for the Ring Magnets of the Synchrotron X-Ray Source at ANL",CH2387-0/87/0000-1526,IEEE PAC87, Washington, pp.1526-1528.
[49]S.C.Snowdon,"Transfer function between magnetic field and excitation current in Main ring bending magnets", FNAL Internal Report,TM-325,1971.

Appendix All-in-One Circuit Diagram of the HIMAC Power Supply

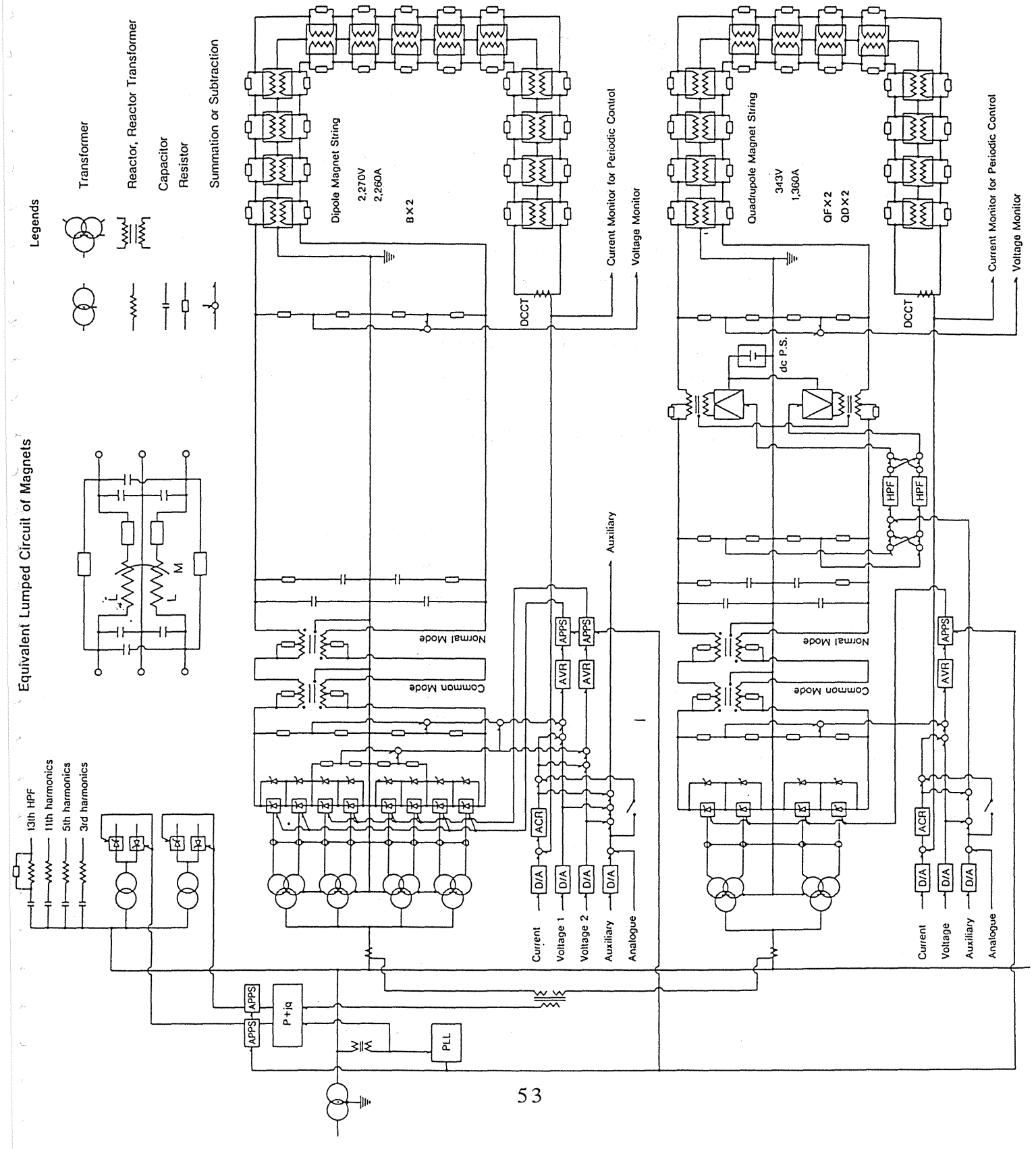

Appendix - HIMAC Parameters

Power Supplies

Relative Ripple Goal (ppm in RMS)		
Quadrupole Magnet	3	(0.3 [1] achieved)
Bending(Dipole) Magnet**	5 to 10[2]	(0.2 [3]achieved)
Stability Goal (ppm)	20	
Repetition (Hz)	0.3- 1.5	at 600 MeV/u
Rise/flat top duration(s)(600MeV)	0.7/0.5	at 0.5 Hz
Rate of field change (T/s)	1.4	

([1] 0.3 ppm achieved with Bandpass filter,
[2] without Active Filter,[3] with Active Filter)

Rectifier of Bending Magnet Power Supply
8 blocks 6 pulse Thyristor Rectifier, Invertor and Convertor Method
Rectifier of Quadrupole Magnet Power Supply
4 blocks 6 pulse Thyristor rectifier

Filter parameters of Common and Normal Mode

	Dipole	Quadrupole
L_{static}(mH)	2.5	0.5
C_1(mF)	0.4	2
C_2(mF)	2	10
R(Ω)	2.2	0.44
Cutoff Frequency(Hz)	71.2	71.2
$L_{dynamic}$(mH)	0.25	0.5
Power Amp(VA)	(160x120)[4]	100x10

Load	Dipole	Quadrupole
Output Power(MW)	5.13	0.538
Voltage(kV)	2.27	0.32
Current(kA)	2.26	1.35
Total Inductance [5](mH)	633.1	110.8
Resistance(mΩ)	200.2	116.8

[4] Later installed as upgrade. [5] Normal Mode

Static Var Controller	
Method	12 pulse Thyristor Controlled Reactor
Power	8 MVar
Energy (MeV/u)	
(4 He-28 Si, q / A = 1 / 2)	100 - 800
(40A r, q/A <1 / 2)	100 - 600
Average Radius(m)	20.65
Maximum BL(Tm)	9.73
Nomalized Acceptance(πmm.mrad)	
(Horizonta/Vertical)	30/3
Number of Lattice(FODO)	12
Superperiod	6
Betatron Tune(Horizontal/Vertical)	3.75 / 3.25
Number of Bending Magnet	
(Sector type, 3.4 m in length)	12
Curvature (m)	6.5
Number of Quadrupole (0.4 m in length,	
Optimized by End Shaping)	24
Field Gradient (T/m)	0.4 / 7.4
RF system	
Number of Cavity(1 m)	1
Frequency Range(MHz)	1-8
Maximum Accelerating Voltage	
(@1MHz) (kV)	11
Momentum Acceptance(%)	+- 0.2
Momentum Spread of Injcted Beam (%)	+- 0.1
Master Oscillator	Digital Synthesizer
Average Vaccum Pressure(Torr)	5×10^{-9}
Baking Temperature(Degree)	200
Vaccum Duct Material	SUS 316
Dipole Vaccum Duct	
(11.5 mm Rib Enforced Duct	
0.3 mm in thickness)	(280 x 63)
Quadrupole Duct	(246 x 100)
(R40mm, 3mm in thickness)	

Multiturn Injection	
Emittance of Injected beam (normalized) (πmm-mrad)	1.5
Acceptance(normalized) (π mm-mrad)	30 / 3
Number of Turns	10-30
Injection Period(ms)	70-240
Slow Extraction	
Third Integer extraction Tune ν_x	11/3
Extraction Period(s)	0.4(0.5Hz)
Maximum Beam Emittance(absolute) (Horizontal/Vertical)(π mm-mrad)	10/10

Lattice of HIMAC
(ν_x=3.75, ν_y=3.25)